12-2016

A GIS Approach to Modeling Groundwater Levels in the Mississippi River Valley Alluvial Aquifer

Josef Orion Lilly
University of Arkansas, Fayetteville

A GIS Approach to Modeling Groundwater Levels in the Mississippi River Valley Alluvial Aquifer

A thesis submitted in partial fulfillment
of the requirements of the degree of
Master of Science in Geography

by

Josef Orion Lilly
University of Arkansas
Bachelor of Arts in International Relations, 2013

December 2016
University of Arkansas

This thesis is approved for recommendation to the Graduate Council.

Dr. Jason Tullis
Thesis Director

Dr. W. Fred Limp
Committee Member

Dr. J. Vaughn Skinner Jr.
Committee Member

ABSTRACT

Groundwater depletion, a subject of growing concern for a significant portion of Arkansas, may lead to future economic challenges for the Arkansas Delta region. The Mississippi River Valley Alluvial Aquifer is the uppermost aquifer and features the largest groundwater capacity in the Mississippi Embayment Aquifer System. The Mississippi River Valley Alluvial Aquifer, commonly referred to as the "alluvial aquifer", spans 53,000 km^2 underlying portions of Arkansas, Kentucky, Louisiana, Mississippi, Missouri, Illinois, and Tennessee. As the alluvial aquifer trends southward for approximately 250 miles alongside the Mississippi River, its geographical extent ranges from 50 to 125 miles wide. There is a considerable correlation associated with groundwater withdrawals level declines and the expansion of rice production, which was introduced to the Arkansas Grand Prairie in 1896 when W.H. Fuller returned from a hunting trip in Louisiana with rice seed. By 1916, the rate at which groundwater was being withdrawn already exceeded the natural recharge rate on the Grand Prairie. Mainstream GIS software provides a means for the modeling of groundwater levels through various spatial interpolation methods. Interpolation is the process of estimating unknown values in the form of a continuous surface, which utilizes observed values with known locations. With the growing concern of groundwater depletion in Arkansas, determining what is the most appropriate spatial interpolation method for producing accurate and reliable modeling of groundwater levels is essential. In addition, increased scrutiny on water resources is inevitable, and determining what is the most appropriate spatial interpolation method for producing accurate and reliable modeling of groundwater levels is essential. Based upon the results of two types of cross-validation for five separate years, ordinary kriging is the most appropriate interpolation method for generating groundwater level estimations for this particular study area. Simple

kriging and empirical Bayesian kriging also provide suitable methods for producing groundwater level estimations for the Mississippi River Valley Alluvial Aquifer.

ACKNOWLEDGEMENTS

I would like to express my special appreciation and thanks to my advisor and professor, Dr. Jason Tullis for his encouragement, support, and advice on my graduate research as well as on my career. I would also like to express my appreciation to my professor and thesis committee member, Dr. W. Fred Limp and to my thesis committee member Dr. J. Vaughn Skinner Jr.

DEDICATION

This thesis is dedicated to my wife, Wendy for all the patience and support she has given me throughout my graduate research.

TABLE OF CONTENTS

LIST OF FIGURES

LIST OF TABLES

1. Introduction and Background

Groundwater depletion, a subject of growing concern for a significant portion of Arkansas, may lead to future economic challenges for the Arkansas Delta region. To a lesser degree, there is the potential that exhaustive groundwater withdrawals in the Gulf Coastal region could also result in regional water conservation issues. According to a United States Geological Survey (USGS) report regarding nationwide water usage in 2010, groundwater withdrawals in Arkansas accounted for over ten percent of the total groundwater withdrawals in the United States during that particular year (Maupin et al., 2014, p. 9). The exhaustive rate of withdrawals, resulting primarily from water-intensive agriculture irrigation practices, has led to the depletion of groundwater levels in the Mississippi Embayment Aquifer system to occur at rates that greatly exceed the rates of natural groundwater recharge. This study aims to determine which spatial interpolation method is the most appropriate for modeling groundwater levels in The Mississippi River Valley Alluvial Aquifer.

1.1. Mississippi Embayment Aquifer System

The Mississippi Embayment Aquifer System underlies eight southern states and encompasses an area of approximately 202,000 km^2, while spanning from southern Illinois to the Gulf of Mexico (Konikow, 2013, p. 21). The aquifer system consists of six separate aquifers as well as three confining units (Konikow, 2013, p. 21). These aquifers are formed by extensive water-bearing assemblages of gravels and sands, separated by less permeable beds of clay (Konikow, 2013, p. 21).

1.1.1. Mississippi River Valley Alluvial Aquifer

The Mississippi River Valley Alluvial Aquifer is the uppermost aquifer and features the largest groundwater capacity in the Mississippi Embayment Aquifer System (Czarnecki et al.,

2002, p. 1). The Mississippi River Valley Alluvial Aquifer, commonly referred to as the "alluvial aquifer", spans 53,000 km^2 underlying portions of Arkansas, Kentucky, Louisiana, Mississippi, Missouri, Illinois, and Tennessee (Czarnecki et al., 2003, p. 2). As the alluvial aquifer trends southward for approximately 250 miles alongside the Mississippi River, its geographical extent ranges from 50 to 125 miles wide (Czarnecki et al., 2003, p. 2).

While the alluvial aquifer underlies the vast majority of the Arkansas Delta region, Crowley's Ridge is a noteworthy exception. Trending from the Arkansas-Missouri border southward to Phillips County, this elongated geological feature restricts the flow of groundwater between the eastern and western lowlands throughout the majority of its extent (Mahon and Ludwig, 1990, p. 3). The ridge averages around 10 miles in width; however, it serves as a significant obstruction to the flow of groundwater and groundwater levels vary greatly between sides (Mahon and Poytner, 1993, p.6).

A confining unit composed of silt, clay, and fine sand, commonly referred to as the clay cap, overlays the alluvial aquifer. The clay cap, shown in Figure 1, generally extends from 20 to 50 feet below the land surface; however, it reaches depths of 80 feet in the Grand Prairie (Czarnecki et al., 2003, p. 2) (Mahon and Poytner, 1993, p.6). The nature of the confining unit is an important variable to the natural rate of recharge to the aquifer.

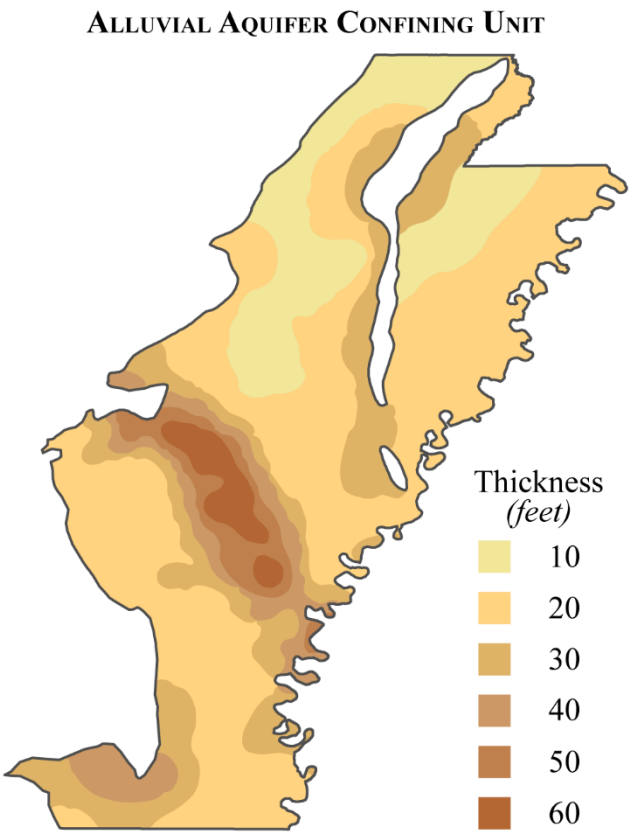

Figure 1. The thickness of the alluvial aquifer's overlying confining unit, also referred to as clay cap, represented in feet. The natural rate of recharge to the aquifer is directly related to the thickness of the confining unit. (USGS, "Ground Water Atlas of the United States")

The vertical thickness of an aquifer refers to depth of the extensive water-bearing assemblages, which forms the aquifer. In Arkansas, the vertical thickness of the alluvial aquifer varies from 15 and 195 feet. The vertical thickness of the alluvial aquifer north of the Arkansas River averages around 100 feet, while south of the Arkansas River, the average vertical thickness is around 85 feet. In turn, the alluvial aquifer serves a substantial source of groundwater (Mahon and Ludwig, 1990, p. 1). Additionally, the alluvial aquifer features hydraulic conductivity values that range from 120 to 390 feet per day (Mahon and Ludwig, 1990, p. 1). However, because of significant declines in water levels over the past decades, primarily resulting from rice irrigation practices, the general condition of the alluvial aquifer has deteriorated.

1.1.2. GROUNDWATER DEPLETION IN THE ALLUVIAL AQUIFER

As agricultural practices developed on the Arkansas Grand Prairie during the late eighteenth century, the demand for reliable water sources also increased. In turn, farmers who lacked access to adequate surface water sources for irrigation began withdrawing groundwater from the alluvial aquifer for irrigation purposes. By the 1890s, the use of wind-powered irrigation wells was already a common practice throughout the Grand Prairie (Gates, 2005, p. 399). The Grand Prairie experienced consecutive years of drought in 1893 and 1894, which stimulated additional farmer interest in groundwater retrieval from the alluvial aquifer. Shortly after, primitive forms of irrigation pumps powered by wood-fueled steam engines were introduced on the Grand Prairie. By 1908, these pumps had already improved enough in performance and efficiency to supply Grand Prairie farmers with yields higher than 1,500 gallons per minute (Gates, 2005, p. 400).

By 1916, the rate at which groundwater was being withdrawn already exceeded the natural recharge rate on the Grand Prairie (Gates, 2005, p. 402). Over the next two decades, groundwater retrieval capabilities were further enhanced with the introduction of diesel and electric well pumps on the Grand Prairie, which led to the first documented groundwater level decline in the alluvial aquifer to occur in 1927 (Engler et al., 1945, p. 21). Only Grand Prairie farmers equipped with high yield wells were prepared for the drought of 1930 when Grand Prairie farmers still attained above average rice harvests despite the challenging conditions (Gates, 2005, p. 406). The extreme heat and the lack of precipitation resulted in heavy pumping on the Grand Prairie. Consequently, the USGS reported that well levels declined in 1930 by an average of 1.8 feet on the Grand Prairie (Gates, 2005, p. 406). Contrastingly, the 1930 drought

resulted in a considerable portion of the crops produced in other regions of the Arkansas Delta to fail (Gates, 2005, p. 406).

According to a 1970 Arkansas Geological Commission water usage report, groundwater withdrawals were already occurring at rates of 1,064 million gallons per day in Arkansas for irrigation purposes alone (Halberg, 1972, p.12). Arkansas County, located in the heart of the Grand Prairie, exhibited total water usage rates of 234 million gallons per day according to the report (Halberg, 1972, p. 2). By 2000, the water usage rate from the alluvial aquifer in Arkansas County consisted of approximately 475 million gallons of groundwater per day from wells. (Czarnecki et al., 2002, p. 1).

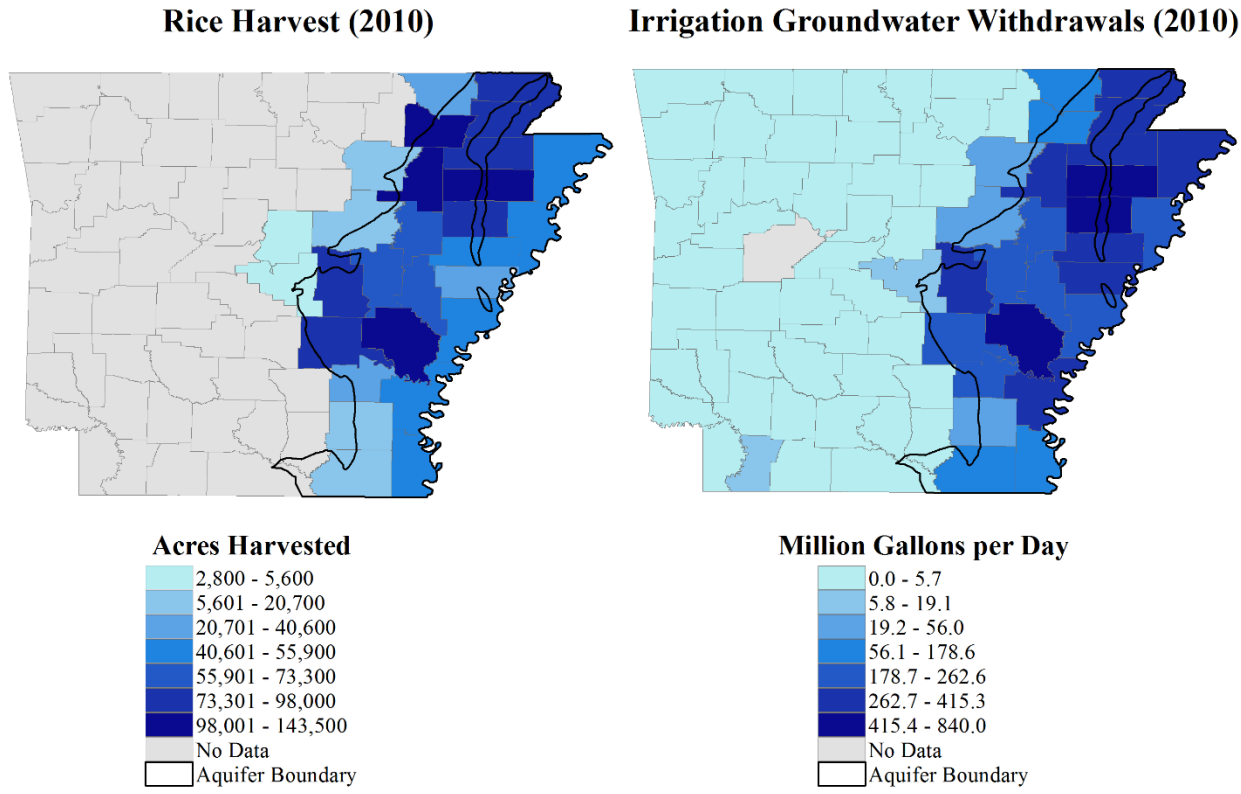

Figure 2. Diptych map displaying acres of rice harvested and groundwater withdrawals for irrigation purposes in 2010. These maps demonstrate a strong correlation between rice production and groundwater withdrawals for irrigation purposes in east Arkansas. (NASS, "Data and Statistics") (USGS, "USGS Water Use Data for Arkansas")

1.2. RICE CULTIVATION

There is a considerable correlation associated with groundwater withdrawals level declines and the expansion of rice production. Rice was introduced to the Arkansas Grand Prairie in 1896 when W.H. Fuller returned from a hunting trip in Louisiana with rice seed (Gates, 2005, p. 396). By 1904, the University of Arkansas agricultural experiment station located in Lonoke had already started rice research (Gates, 2005, p. 396). With much of the Arkansas Delta featuring a substantial groundwater supply, low topographic relief, and poorly drained soils, Arkansas rice production has experienced tremendous growth rates expanding into other regions of Arkansas Delta, particularly northeast Arkansas. Because of the expansion of rice throughout the Arkansas Delta, rice production is now deeply embedded in the economy of eastern Arkansas economy and Arkansas produces around half of the rice grown in the US annually. In 2010, Arkansas rice production experienced record highs when the rice harvest reached 1.785 million acres (Rice Production in Arkansas, n.d.). However, the expansion of rice production, which requires more water than any of the other crops commonly produced in Arkansas, has undoubtedly had a negative impact on Arkansas' groundwater resources. According to a 2010 USGS Arkansas water usage report, an average of 2.95 feet of water was applied per acre during rice production (Pugh and Holland, 2015, p. 20). For comparative purposes, the average irrigation rates for other major crop types include an average of 1.65 feet of water per acre of corn, 1.62 feet of water per acre soybeans, and 1.53 feet of water per acre of cotton (Pugh and Holland, 2015, p. 20). According to the University of Arkansas - Division of Agriculture, the average energy input cost associated with irrigating one acre of rice was $92.92 (Flanders, 2014, p. 2). Comparatively, cotton required the second highest average irrigation energy cost, with one acre of cotton averaging $38.14 of irrigation energy costs (Flanders, 2014, p. 2). The average

input cost associated with energy cost irrigation provides a valuable indication of irrigation rates for the various crops grown in Arkansas; however, this input cost average can also be influenced by variations in the efficiency and type of the irrigation pumps that are used for the irrigation of certain crop types.

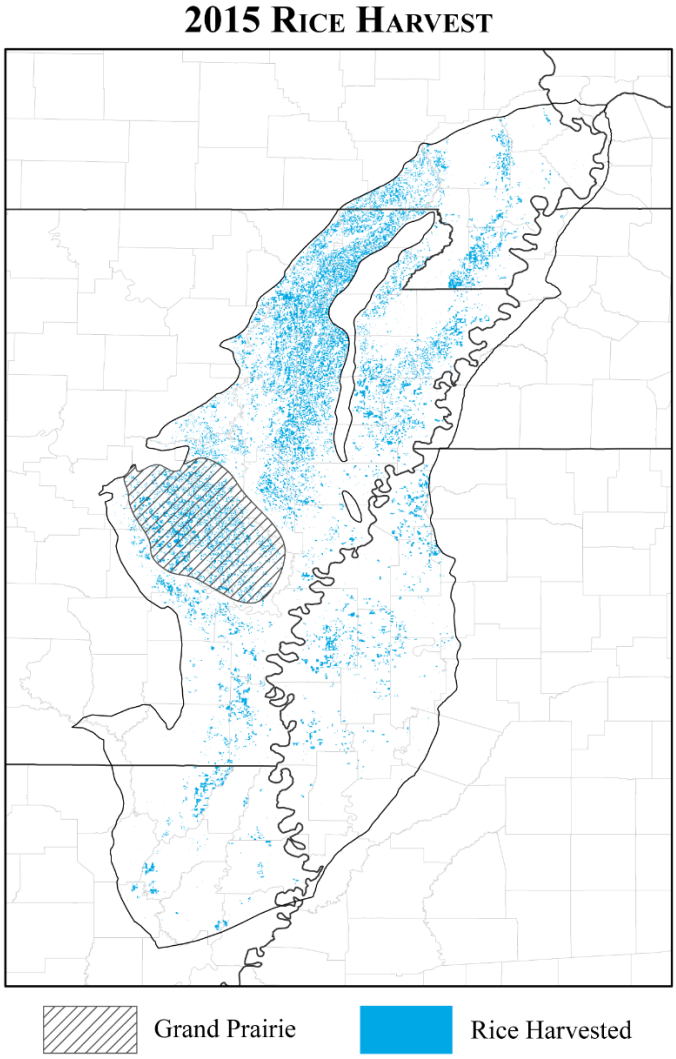

Figure 3. This map displays the distribution of rice production within the extent of the Mississippi River Valley Alluvial Aquifer in 2015. This map demonstrates the expansion of rice production from Grand Prairie to other regions of the Mississippi Alluvial Plain, particularly, the notable expansion into Northeast Arkansas as well as Southeast Missouri (NASS, "CropScape – Cropland Data Layer")

1.3. GEOGRAPHIC INFORMATION SYSTEMS (GIS)

Geographic Information Systems (GIS) is a computer technology that provides a means of mapping, visualizing, managing, editing, querying, processing, modeling, and analyzing spatial datasets. The first documented use of Geographic Information Systems as a term occurred in 1968 when a research paper titled "A Geographic Information System for Regional Planning" was published by Dr. Roger Tomlinson (The 50th Anniversary of GIS, 2012). The progression of GIS software programs, methodologies, and technology through the years has led to the successful implementation of GIS in a growing number of fields, such as archeology, law enforcement, transportation, real estate, geology, environmental sciences, agriculture, local government, public services, in addition to countless other fields.

1.3.1. GIS GROUNDWATER MODELING

Increasingly, GIS applications have been utilized for purposes related to water resources and hydrology. GIS provides abundant applications within the groundwater field, due to the ability of GIS applications to display spatially various pertinent features as directed by the user, along with the ability to apply model components or processes from one study area to another. In addition to the advanced modeling capabilities associated with GIS software, they also provide an appropriate platform for managing hydrological databases. GIS software is also frequently utilized to monitor and manage groundwater resources. Monitoring and management practices often include hydrogeological modeling, modeling of spatial continuous groundwater data, calibrating of aquifer models, investigating groundwater storage capabilities, as well as establishing a network for groundwater data collection (Khazaz et al., 2015, p. 632).

1.3.2. SPATIAL INTERPOLATION

Mainstream GIS software provides a means for the modeling of groundwater levels through various spatial interpolation methods. Interpolation is the process of estimating unknown values in the form of a continuous surface, which utilizes observed values with known locations (Bohling, 2005, p. 2). With the growing concern of groundwater depletion in Arkansas, increased scrutiny on water resources is inevitable, and determining what is the most appropriate spatial interpolation method for producing accurate and reliable modeling of groundwater levels is essential. As demonstrated by numerous relevant case studies, which will be discussed in detail later on, there is not yet a consensus among scholars regarding which spatial interpolation tool is the most appropriate for modeling groundwater levels. Furthermore, variations in a datasets nature will also have a considerable impact on the reliability and performance of each particular interpolation method within a given case study.

Spatial interpolation methods can be categorized as being either probabilistic or deterministic. In probabilistic spatial interpolation methods, the degree of similarity observed is taken into consideration while computing weight values (Khazaz et al., 2015, p. 635). In contrast, the influence of observed point data is directly related to the distance of the observed point data from the particular point being estimated during deterministic methods. However, all spatial interpolation methods assign weighted averages for observed values as well as utilize the same formula during estimation (Khazaz et al., 2015, p. 634). The primary difference between all spatial interpolation methods is the varying means for assigning weight values to point data within the study area. Weight values refer to the intensity of influence of the observed point values throughout estimation.

The estimation formula utilized by spatial interpolation methods is listed as:

$$F(X_p) = \sum_{i=1}^{m} \lambda_i F(X_i)$$

1.3.2. 1. KRIGING INTERPOLATION METHODS

Kriging, named after South African mining engineer D.G. Krige, is a spatial interpolation technique that utilizes geostatistical methods as a means of estimating a continuous surface of values. Krige as well as Georges Matheron, a French geomathematician, developed kriging methods for interpolation practices within the mining industry (Burrough and McDonnell, 1998, p.133). One way that kriging (a probabilistic method) varies from the other spatial interpolation methods is that kriging methods take into consideration how similar estimated values are expected to be in relation to known values, whereas deterministic interpolation methods only perform calculations in regards to the spatial coverage of a dataset. During kriging calculations, weights are assigned utilizing data-driven weighting functions. Kriging techniques rely on covariance values amongst known points, along with covariance values between known points and the points to be estimated (Bailey and Gatrell, 1995, p. 183). Kriging methods employ the regionalized variable theory; therefore, notions of stochastic aspects of spatial variation are applied during the calculation of interpolation weights (Burrough and McDonnell, 1998, p. 303). Kriging interpolation techniques, frequently employed for modeling features in geosciences, prove to be optimal methods when a dataset features a spatially correlated or directional bias. One advantage associated with utilizing kriging methods are that derived estimations are provided along with an output variance of prediction raster, which exhibits the degree uncertainty during quantification (Jamil et al., 2011, p. 9).

Before selecting a variation of kriging for the purpose of conducting spatial interpolation processes, one must be aware that kriging has several assumptions about a dataset. First, kriging techniques assume, likewise with all interpolation techniques, that the respective dataset is

spatially continuous (Childs, 2004). Spatially continuous can be described as the notion that every point within a specified area of interest contains a value. As previously stated, kriging also assumes that a dataset is spatially autocorrelated. This assumption is demonstrated by the notion that data located within closer proximities will yield more comparable values than would data located at greater distances. Another fundamental assumption of kriging is that data is stationary; therefore, the estimation of values will rely on distances between established values as opposed to their actual location. Additionally, kriging assumes a dataset as having an even distribution without profound clustering. However, it is possible to address this particular assumption through kriging's declustering options (Childs, 2004). In general, kriging techniques estimate a constant value average across a surface; therefore, most kriging variations assume that global trends are not present within a dataset (Childs, 2004).

There are numerous variations of kriging methods that can be utilized for generating a continuous surface of values. A widely used form of kriging is ordinary kriging, which employs the regionalized variable theory during estimation, while it assumes a constant yet unknown mean throughout the area of interest. (Burrough and McDonnell, 1998, p. 303). Simple kriging, another well-known form of kriging, can be easily distinguished from other kriging methods by its assumption that a sample's mean is both constant and known (Olea, 2009, p. 133). Universal kriging is another form of kriging widely used in practice, where systematic variation modeled by a trend or drift surface is taken into consideration during calculations (Burrough and McDonnell, 1998, p.149). Stratified Kriging is a unique kriging method, with stratified kriging producing a surface of values that represent strata or divisions that form separate classes across a surface (Burrough and McDonnell, 1998, p. 147). Block kriging is another distinctive form of kriging, which predicts a surface of values where estimated values are represented through

square block units (Burrough and McDonnell, 1998, p. 143). Co-kriging takes one or more additional variables into consideration when generating a continuous surface of values. This kriging method serves as a constructive alternative if there are any potential concerns associated with undersampling of the primary variable (Burrough and McDonnell, 1998, p. 147). Other methods of kriging include, but are not limited to multivariate kriging, probastic kriging, indicator kriging, and disjunctive kriging. Nonetheless, simple kriging, ordinary kriging, universal kriging, and empirical Bayesian kriging are the forms of kriging that will be addressed in this respective case study.

Simple kriging, which has roots that predate geostatistics, was the earliest form of kriging (Olea, 2009, p. 156). Burrough and McDonnell define simple kriging as "an interpolation technique in which the prediction of values is based on a generalized linear regression under the assumption of second order stationary and a known mean" (1998, p. 305). Simple kriging may provide optimal results in the presence of a mean that is both known and constant; however, this particular kriging method is seldom utilized in practice (Bailey and Gatrell, 1995, p. 188). Burrough and McDonnell claim that the restrictive nature of simple kriging's assumption of second order stationary could prove to be a potential shortcoming of a simple kriging method (1998, p. 144). Meanwhile, R.A. Olea states that simple kriging is also restricted by another assumption that is distinctive to simple kriging, which is the assumption that the mean is both known and constant (2009, p.133). Nevertheless, a relevant case study located in northwest China, which will be discussed in more detail in the next section, concluded that simple kriging served as the optimal interpolation method for estimating groundwater levels in that particular study area (Sun et al., 2009).

Ordinary kriging was initially formulated for the purpose of improving upon simple kriging. The primary distinction between simple kriging and ordinary kriging methods is the assumption that the mean is constant; however, unknown over the complete area of interest (Bailey and Gatrell, 1995, p. 194). This assumption suggests that there are no major trends present within a dataset, which results in the estimator being unbiased (Olea, 2009, p. 156). An additional consequence of this no assumption is that ordinary kriging generates surface predictions utilizing localized means (Bailey and Gatrell, 1995, p. 196). However, the assumption of a constant mean is a notion that has faced criticism from a variety of scientists. Ordinary kriging's point estimation relies on the regionalized variable theory, and a fitted variogram model is utilized for calculating prediction weights (Burrough and McDonnell, 1998, p. 303).

Universal kriging can be described as kriging that features a built in trend (Burrough and McDonnell, 1998, p. 149). In this kriging method, a regression equation is incorporated into calculations in order to account for an external trend present within a dataset (Burrough and McDonnell, 1998, p. 149). Universal kriging, which assumes that that mean is neither known nor constant, is a very complex kriging method that should be used with caution (Olea, 2009, p. 193). Universal kriging models errors for autocorrelation, instead of assuming that the resulting errors are independent (Bailey and Gatrell, 1995, p. 196). Universal kriging will produce optimal results when a dataset's values exhibit clear and systematic variation (Olea, 2009, p. 193). This particular technique is widely used in environmental science practices, where prominent spatial trends are generally present within datasets.

Empirical Bayesian kriging is a kriging method where the task of constructing a semivariogram that appropriately represents a dataset is automated. In contrast to other kriging

methods that utilize a single semivariogram during estimation, an empirical Bayesian kriging employs several semivariograms when generating a surface (Krivoruchko, 2012). The first step in empirical Bayesian kriging is estimating a single semivariogram model (Krivoruchko, 2012). During the following step, new values are estimated at input data locations. Afterwards, a new semivariogram model is generated employing the recently estimated values (Krivoruchko, 2012). Additionally, the second and third steps are repeated numerous times, which results in a spectrum of semivariograms (Krivoruchko, 2012). Another noteworthy feature of empirical Bayesian kriging is the data transformation option.

1.3.2.2. Inverse Distance Weighting (IDW)

Inverse distance weighting or IDW is a local deterministic spatial interpolation method that estimates a continuous surface of values through the weighted averaging of values relevant to values at known positions. In this technique, sample points that are located within a close proximity will have a superior weight during averaging than will points that are located farther away from a particular position. IDW is categorized as being an exact interpolator; as a result, IDW's estimated minimum and maximum values will occur at sample points. IDW has two assumptions that one must be mindful when selecting this technique, which are the assumptions of a dataset being autocorrelated and unclustered (Childs, 2004). Additionally, the presence of outliers in a dataset could create concerns for the performance of an IDW interpolation method. This respective study will employ an IDW interpolation method as well as an IDW with barriers interpolation method. The only notable difference between the two interpolation methods is the ability to input an absolute barrier, which could prove to be very valuable as Crowley's Ridge can be accurately represented as a physical barrier that restricts the flow groundwater within the study area.

1.3.2.3. RADIAL BASIS FUNCTIONS

Radial Basis Functions (RBF) are a set of exact spatial interpolators, which vary from other types of interpolation because all forms of RBF interpolation methods will generate an estimated surface that intersects every known value in the study area (How Radial Basis Functions (RBF) work, 2007). Nonetheless, RBF interpolation methods will produce estimated surfaces that vary in appearance and estimation quality. This case study will address the performance of six RBF forms of interpolation, which are regularized spline, tension spline, thin plate spline, spline with barriers, multiquadric functions, and inverse multiquadratic functions.

A simple explanation of how spline interpolation works would be illustrated by the idea of stretching a flexible surface through all of the known values located within a particular study area (Childs, 2004). Utilizing slope calculations spline interpolation generates a smooth surface that represents spatial variation, therefore if spatial clustering or extreme outliers have a considerable presence within a dataset then a spline method would not serve as a reasonable interpolation method (Childs, 2004). Additionally, sudden changes in values, referred to as break points, will produce performance concerns for spline interpolation methods. However, being an exact interpolator, a spline method could prove to be a reasonable method if the priority is the accurate estimation of a surface's high and low values.

A regularized spline could be described as being elastic in nature and will generally generate a smoother surface where changes occur at a more gradual rate compared to the rate of changes in a surface produced with tension spline (Childs, 2004). A regularized spline could potentially predict unknown values that fall outside of the range of values established by the known values. In comparison, tension spline will generally produce a surface that is flatter and more rigid in nature (Childs, 2004). Additionally, the predicted values generated with tension

spline tend to exhibit a stronger correlation to the range of known values. Alternatively, thin plate spline uses localized smoothing averages to generate a spline surface without the excessively high and low values that commonly result from other spline methods (Burrough and McDonnell, 1998, p. 120). The spline with barriers interpolation method uses known values and absolute barriers to generate a minimum curvature surface by employing a one-directional multigrid technique (How Spline with Barriers works, 2011).

Ronald Hardy, seeking to improve upon polynomial interpolation techniques, invented multiquadric interpolation in 1968 in order to generate topographic maps (Chenoweth, 2009, p. 58). According to Chenoweth, Hardy named the interpolation method multiquadric after the 'quadric' surface that was generated (2009, p. 60). Today multiquadric interpolation is still commonly used to produce topographic maps and has proven to succeed in circumstances where polynomial interpolation techniques have failed (Chenoweth, 2009, p. 58). Chenoweth goes on to claim that multiquadric interpolation can produce an accurate surface model with scattered known point values (2009, p. 59). Inverse multiquadric interpolation utilizes a smaller degree of freedom; therefore, this method is believed to be more efficient and generate more accurate estimation (Javaran and Khaji, 2012, p.1)

1.3.2.4. POLYNOMIAL INTERPOLATION

Global polynomial interpolation, commonly referred to as trend surface analysis, is an interpolation method that addresses potential relationships between variables and the spatial locations of sample points (Burrough and McDonnell, 1998, p. 109). This method could prove to be valuable for modeling significant variations of the mean value in a spatially continuous dataset (Bailey and Gatrell, 1995, p. 168). Trend surface analysis relies on a polynomial function to produce a smooth surface model relative to the known values of the sample points. The

polynomial equation utilized during calculations is a two-dimensional polynomial equation of the first, second, or higher degree (Yao et al., 2013, p. 2). The general idea of a trend surface analysis can be explained as the idea of fitting a piece of paper through the observed data points. Burrough and McDonnell claim that one advantage of this interpolation method is the simplicity of calculations (1998, p. 109). However, it is also stated that a trend surface analysis is commonly utilized for locating areas within a study area that deviate from the general trend of a dataset (Burrough and McDonnell, 1998, p. 109). The resulting outcome could assist in preparing a dataset before utilizing another interpolation method through providing an effective means for identifying noise within a spatial dataset. Furthermore, trend surface's polynomial functions can be employed for displaying any potential drifts exhibited by a spatial dataset (Khazaz et al., 2015, p. 636). For groundwater related purposes, drifts demonstrated by a trend surface analysis could provide potentially valuable insight into the various directions of groundwater flow within a particular study area (Khazaz et al., 2015, p. 636).

The local polynomial interpolation (LPI) method features characteristics from both inverse distance weighting and global polynomial interpolation techniques. A surface generated using LPI will represent both localized behaviors and variations in the overall trend of a spatial dataset (Yao et al., 2013, p. 2). This method's estimation relies solely on the sample points that fall within a specific neighborhood. However, there is some overlap between search neighborhoods and a specific search neighborhood's estimated value is assigned to the center of that particular search neighborhood.

In addition, the performance of kernel interpolation with barriers and diffusion interpolation with barriers will also be addressed in this case study. Kernel interpolation with barriers is a first order polynomial variant of LPI that features an optional absolute barriers

parameter. A noteworthy difference between the methods is that kernel interpolation utilizes the shortest distance between points in order to improve estimation accuracy around any absolute barriers defined within an area of interest (Kernel Interpolation with Barriers, n.d.). Diffusion interpolation with barriers refers to kernel interpolation utilizing the Gaussian Kernel, which is also the fundamental solution of the heat equation (How Diffusion Interpolation with Barriers works, n.d.).

1.3.2.5. TRIANGULAR IRREGULAR NETWORK (TIN)

Triangular Irregular Network (TIN) is a method for modeling spatial data that utilizes tessellated triangles for representation purposes. Numerous tessellation, or tiling, methods may be utilized in a TIN representation. The resulting 'tiles' are commonly referred to as Thiessen Polygons or Voronoi (Bailey and Gatrell, 1995, p. 156). Two of the most commonly utilized tessellation techniques are Dirichlet tessellation and Delaunay triangulation. A primary concern associated with this particular interpolation method would be its inability to estimate any values outside the spatial extent of known values.

1.4. SPATIAL INTERPOLATION STATISTICAL ACCURACY ASSESSMENT

1.4.1. CROSS-VALIDATION

In this study, each method's estimated surface will be assessed and compared utilizing cross-validation techniques. Cross-validation serves as an appropriate means for assessing an interpolated surface's accountability through the calculation of statistical errors produced during estimation (Olea, 2009, p. 241). Additionally, cross-validation's statistical analysis provides a way to comparatively analyze the performance of multiple spatial interpolation methods.

During cross-validation, observations are partitioned into two separate subsets, which are referred to as the training set and the test set. The known training set is utilized by a model to generate estimations, while the unknown test set is withheld. Afterwards, the test set is employed for testing the performance of a model. Cross-validation methods can be categorized as being either exhaustive cross-validation or non-exhaustive cross validation. The means of partitioning observations is the distinguishing characteristic between the two categories of cross-validation. Exhaustive cross-validation methods address all possible partitions within a set of observations, whereas non-exhaustive cross-validation methods do not utilize these extensive partitioning techniques.

1.4.1.1. K-Fold Cross-Validation

K-fold cross-validation, a widely used non-exhaustive cross validation method, partitions observations equally into *k* subsets, with *k* representing the number of partitioned subsets (Ounpraeuth et al., 2012, p.1). Estimations are performed *k* number of times with each subset serving as the test set one time; consequently, every observation is used once for validation purposes (Ounpraeuth et al., 2012, p.1). While the *k* parameter is defined by the user; however, ten fold cross-validation is commonly used in practice (Ounpraeuth et al., 2012, p.2).

1.4.1.2. Leave-one-out Cross-Validation

Leave-one-out cross-validation is an exhaustive cross validation method where every observation is removed once for the purpose of validating a model (Burrough and McDonnell, 1998, p. 300). In this method, estimations are generated for the dropped values utilizing a training set that is defined as $n - 1$, where n represents sample size and -1 represents the removed observation. The resulting statistics regarding the prediction errors observed during leave-one-out cross-validation serves as an excellent way to evaluating an estimator's accountability;

however, it must be noted that spatial clustering could result in unrepresentative prediction error (Olea, 2009, p. 244). This can be illustrated by the notion that dropped observations located within a cluster would be expected to exhibit prediction errors that are uncharacteristically low in comparison to the observations that are dispersed throughout a study area.

1.5. STATEMENT OF THE PROBLEM

Historically, groundwater resources in Arkansas have been heavily relied on to supply the large volumes of water necessary for the water-intensive agricultural practices that are common in the Arkansas Delta region. The exhaustive demands for groundwater in Eastern Arkansas have resulted in the formation and expansion of two massive cones of depression in the potentiometric surface, which has reduced water quality and yields for wells completed in the affected areas (Czarnecki et al., 2003, p.1). Around the Arkansas Delta, a number of additional smaller cones of depressions are forming or have already formed regionally throughout the alluvial aquifer. Nonetheless, the 2010 USGS nationwide water usage report reveals that groundwater usage rates in Arkansas continue to rank amongst the highest in the nation (Maupin et al., 2014, p. 9). Disturbingly, the overwhelming majority of groundwater withdrawals in Arkansas are supplied by wells completed in the alluvial aquifer. In 2010, approximately 97 percent of the total amount of groundwater withdrawn in Arkansas was supplied by wells completed in the alluvial aquifer (Pugh and Holland, 2010, p. 27).

The alluvial aquifer has faced several long-term impacts, which are the consequences of several decades' worth of excessive groundwater withdrawals. The long-term availability of the alluvial aquifer as a reliable groundwater source will require both groundwater and surface water resources to be managed in an extensive, sustainable, and efficient manner (Clark et al., 2013, p. 1). The ability to effectively and reliably monitor groundwater levels will undoubtedly prove to

be essential in making effective and confident groundwater management decisions (Khazaz et al., 2015, p. 632). Generally, the spatial coverage of in situ groundwater measurements is limited, because of the considerable cost associated with conducting such measurements (Khazaz et al., 2015, p. 632). Spatial interpolation provides an effective means for employing the available network of spatially referenced of in situ groundwater measurements in order to estimate a continuous surface model of groundwater levels. A variety of spatial interpolation methods have been utilized for modeling groundwater depths and each method has a variety of assumptions related to the behavior of the data. Therefore, a considerable amount of the performance of a particular spatial interpolation method is directly related to the behavior of a dataset. Comparative research into the performance of various spatial interpolation methods within the respective study area has the potential to influence groundwater policies and management (Khazaz et al., 2015, p. 633). The primary purpose of this study is to conduct a comparative analysis on the statistical accuracy of the nine previously discussed spatial interpolation methods. The spatial interpolation methods will be subject to a comparative performance assessment based upon cross-validation and a variety of statistical accuracy indicators.

Subsequently, this study will concisely investigate any spatial and temporal trends in the fluctuations of the alluvial aquifer's groundwater levels among five-year periods based on the groundwater level surfaces generated by the spatial interpolation method established as the optimal method for the study area. Additionally, this study seeks to employ any trends exhibited by the resulting surface models in order to generate a future groundwater surface model of forecasted values in relation to the ongoing trends and current rate of withdraw in the alluvial

aquifer. This model would serve as an effective tool for conveying the potential consequences if the rates of groundwater exploitation in the alluvial aquifer are sustained.

In addition, this study will assess the relation of the fluctuation in groundwater levels to the associated rate of groundwater withdrawals at the county level. The average groundwater level change over five years will be calculated for each county within the study area and compared to the respective rate of groundwater usage in the particular county. This study will seek to determine if the majority of the counties located within the study area exhibit a similar interaction between changes in groundwater level and the varying rates of groundwater withdrawals associated with particular counties. The study will also seek to determine if each county demonstrates a comparable correlation of the interaction between the two variables through a variety of five-year time periods. Furthermore, if the interaction between the two variables exhibits consistent correlations at the county level through the varying time periods, then sustainable rates for groundwater withdrawals at the county level could possibly be developed accordingly. Components from this segment of the study could potentially be modified and further developed in order to produce county specific groundwater policies.

1.5.1. RESEARCH QUESTIONS AND HYPOTHESIS

The primary research question under investigation in this study is establishing which spatial interpolation method serves as the optimal method for modeling groundwater levels in the alluvial aquifer. I hypothesize that the probabilistic spatial interpolation methods, ordinary kriging, simple kriging, and universal kriging, will produce superior groundwater surface estimations compared to surface estimations produced by deterministic methods.

A secondary research question would be, have the fluctuations in the alluvial aquifer's groundwater levels exhibited a noticeable general trend of decline in recent history? I

hypothesize that while several of the measurements sites have actually experienced increased groundwater levels, the overwhelming trend of groundwater decline will be visibly obvious when displaying groundwater changes throughout each of the respective five year periods. A recent ten year monitoring study of groundwater level changes in the alluvial aquifer was conducted by the USGS, Arkansas Natural Resources Commission (ANRC), or the Natural Resources Conservation Service (NRCS) and surprisingly the study concluded that around 23.7 percent of groundwater measurement sites actually experienced an increased groundwater level in comparison to the groundwater levels recorded ten years earlier (Swaim, 2014).

A third research question for this study would be do the majority of the study area's counties exhibit a significantly similar interaction between groundwater level changes and the varying rates of groundwater withdrawals associated with particular counties. I hypothesize that there will be there will indeed be a general correlation in relationship between the interactions of the two variables; however, I anticipate that the degree of correlation in the relationship of the two variables in the various counties will exhibit moderate fluctuations.

2. LITERATURE REVIEW

Spatial interpolation techniques performed through various GIS platforms have provided a reliable and effective means for the spatial representation and monitoring of groundwater levels. However, as a number of relevant case studies demonstrate, there is not a general consensus regarding which spatial interpolation technique provides the most suitable for generating groundwater depth surface models. Additionally, there is also variation in the statistical methods employed for evaluating the accuracy of the resulting groundwater surface models.

2.1. SPATIAL INTERPOLATION METHODS

A case study that conducted a comparative evaluation of spatial interpolation methods for modeling groundwater levels in the Wuwei oasis located in Northwest China concluded that ordinary kriging is most suitable interpolation method for interpolating groundwater surface models in the particular study area (Yao et al., 2013, p. 9). However, the article quickly acknowledges that there are a number of limitations associated with ordinary kriging that one must be mindful of (Yao et al., 2013, p. 9). The case study claims that the principle drawback of ordinary kriging is the smoothing effect, which is described in the article as being a "decreased variation of estimates" (Yao et al., 2013, p. 9). In the respective case study, the smoothing effect notion is demonstrated by the ordinary kriging derived surface model yielding a lower standard deviation than the standard deviation that was yielded by the sampling points measurements (Yao et al., 2013, p. 9). The presence of the smoothing effect is also revealed by a reduced range of values in the ordinary kriging derived surface model compared to the range of values that were observed at the actual sampling points (Yao et al., 2013, p. 9). The case study addressed the smoothing effect with the technique established in Yomamoto's journal article "Correcting the

Smoothing Effect of Ordinary Kriging Estimates" (Yao et al., 2013, p. 9; Yomamoto, 2005). Yao et al. concluded that Yomamoto's method productively corrected the smoothing effect associated with ordinary kriging (2013, p. 9).

Charoenpong et al.'s "Impacts of Interpolation Techniques on Groundwater Potential Modeling Using GIS in Phuket Province, Thailand" provides another relevant case study (2012). This particular case study concluded that IDW was the most appropriate interpolation method for modeling groundwater specific capacity in the Phuket Province of Thailand. Groundwater specific capacity (SC) is a measure of well performance which is reliant on the status of groundwater levels. Charoenpong et al. also acknowledges that the power parameter and search radius were both adjusted accordingly to improve the accuracy of the IDW estimates (2012).

Rabah et al.'s journal article "Effect of GIS Interpolation Techniques on the Accuracy of the Spatial Representation of Groundwater Monitoring Data in Gaza Strip" consisted of a comparative evaluation of IDW, ordinary kriging, and tension spline for producing groundwater level surface maps (2011). In this case study, validation as well as cross validation were employed as a means of evaluating the accuracy of each method (Rabah et al., 2011). This respective study concluded that ordinary kriging provided the most appropriate spatial interpolation method for generating groundwater surface maps in the Gaza Strip (Rabah et al., 2011). This conclusion is a result of ordinary kriging yielding the highest correlation values and the lowest residual errors (Rabah et al., 2011).

An additional relevant case study is Kumar and Remadevi's "Kriging of Groundwater Levels – A Case Study", which is a comparative evaluation the performance of ordinary kriging estimates with spherical, exponential, and gaussian semivariogram models for groundwater levels in Rajasthan, India (2006). Both cross validation and jackknifing techniques were

employed as a means of evaluating the accuracy of each model (Kumar and Remadevi, 2006). Utilizing these techniques, Kumar and Remadevi's case study concluded that ordinary kriging's gaussian model served as the most appropriate semivariogram model for generating groundwater surface models in their respective study area (2006).

Salah's "Geostatistical analysis of groundwater levels in the south Al Jabal Al Akhdar area using GIS" employed ordinary kriging with a spherical semivariogram model for generating groundwater surface models (2009). While this case study did not contain a comparative evaluation of the performance of multiple spatial interpolation methods, cross validation was used to assess the accuracy of the generated groundwater surface model (Salah, 2009). Additionally, Salah provides a detailed step by step workflow of his geostatistical analysis carried out in this case study (2009).

Kettle et al.'s case study "Groundwater Depletion and Agricultural Land Use Change in Wichita County, Kansas" employed universal kriging as the means of generating a groundwater surface model (2007). Kettle et al. claims universal kriging was employed in this respective case study because it utilizes weighted local averages in order to estimate unknown values (2007). Wichita County, Kansas server as the study area in Kettle et al.'s case study; however, well measurements within a five-mile buffer were also utilized during estimation in order to improve estimation near the study area boundary (Kettle et al., 2007).

2.1.1. Mississippi River Valley Alluvial Aquifer Groundwater Surface Models

In 2008, the Arkansas Geological Survey (AGS) published a depth to groundwater map for the alluvial aquifer in Arkansas. IDW was the spatial interpolation method that was employed for generating the groundwater surface model relative to the respective map; however, the reason why this particular method was selected as the method for generating the groundwater surface

model was not specified. This particular map was produced through employing ESRI ArcGIS 10.x software and the dataset utilized for generating the estimated surface consisted of groundwater measurements from 684 wells.

The Arkansas Natural Resources Commission produced an alluvial aquifer depth to groundwater estimated surface utilizing nearest neighbor interpolation method. This map was generated utilized ArcGIS 10 and using 2011 data points (Swaim, 2014).

2.2. The Effect of Groundwater Depletion

The alluvial aquifer has already faced with several long-term impacts that have resulted from the long history of excessive groundwater withdrawals throughout the Arkansas Delta. Before the exploitation, the alluvial aquifer demonstrated artesian conditions throughout much of the Grand Prairie, where groundwater levels elevated above the aquifer into the overlying clay cap (Gates, 2005, p. 395). In Arkansas the alluvial aquifer discharged excessive groundwater into the rivers, supplying many of the rivers located on the Arkansas delta with a sizeable portion of their river flow (Czarnecki et al., 2002, p. 3). With critically depleted groundwater levels throughout much of the alluvial aquifer, rivers now serve as a vital recharge source for the aquifer (Czarnecki et al., 2002, p.4). With rivers being relied on more heavily as a primary recharge source for the aquifer, the rate of groundwater depletion is typically accelerated in areas that are located further away from a major river (Czarnecki et al., 2002, p.4). The imbalance of groundwater withdrawals has resulted in the formation and expansion of two extensive cones of depression in the potentiometric surface. These particular cones of depression exist west of Crowley's Ridge around the Cache River bottoms and throughout much of the Grand Prairie. According to a USGS groundwater report published in 2000, smaller potentiometric surface depressions are currently forming in regions of the southern

Arkansas Delta as well (Schrader, 2001, p. 5). Monitoring the development of these potentiometric surface depressions has confirmed that expansion is occurring in both of a radial and vertical fashion (Schrader, 2001, p. 5). There are also growing localized concerns regarding declines in the aquifer's saturated thickness, which refers to the vertical thickness of the zone of saturation within an aquifer, with several isolated areas sustaining saturated thicknesses values that have been reduced to levels below 20 feet (Reed, 2003, p. 2). Groundwater declines have also led to mounting concerns associated with the altered lateral flow of groundwater, reduced groundwater storage capacities, and decreased hydraulic pressure (Czarnecki et al., 2002, p. 3).

3. METHODS AND MATERIALS

3.1. STUDY AREA

This study restricts its focus to groundwater depth measurement completed in the Mississippi Alluvial Aquifer. Although there are five other aquifers in the Mississippi Embayment Aquifer System, the Mississippi Alluvial Aquifer has the largest geographical extent and has experienced the highest levels of groundwater depletion within the aquifer system. Additionally, the Mississippi Alluvial Aquifer features the highest number of groundwater monitoring sites within the aquifer system. Within the study area, the presence of Crowley's Ridge, an elevated topographic feature that rises above the Mississippi Alluvial Plain lowlands, provides an unusual factor that is necessary to address when conducting spatial interpolation. Trending from the Arkansas-Missouri border all the way to Phillips County, this elongated geological feature restricts the flow of groundwater between the eastern and western lowlands throughout the majority of its extent (Mahon and Ludwig, 1990, p. 3). Although there are a number of particular locations where groundwater is free to flow between the otherwise separated lowlands, this topographic boundary must be addressed appropriately prior to any spatial interpolation processes.

While the Mississippi Alluvial Aquifer spans across seven different states and political borders have no direct impact on groundwater levels, the quantity as well as spatial coverage of groundwater data for this respective aquifer in other states is relatively limited. Therefore, this study will focus on assessing the accuracy and reliability of various groundwater models within Arkansas. As a result of the considerable spatial coverage of groundwater measurements in Arkansas, further examination into a county level study area would be possible in the majority of the counties located within the study area.

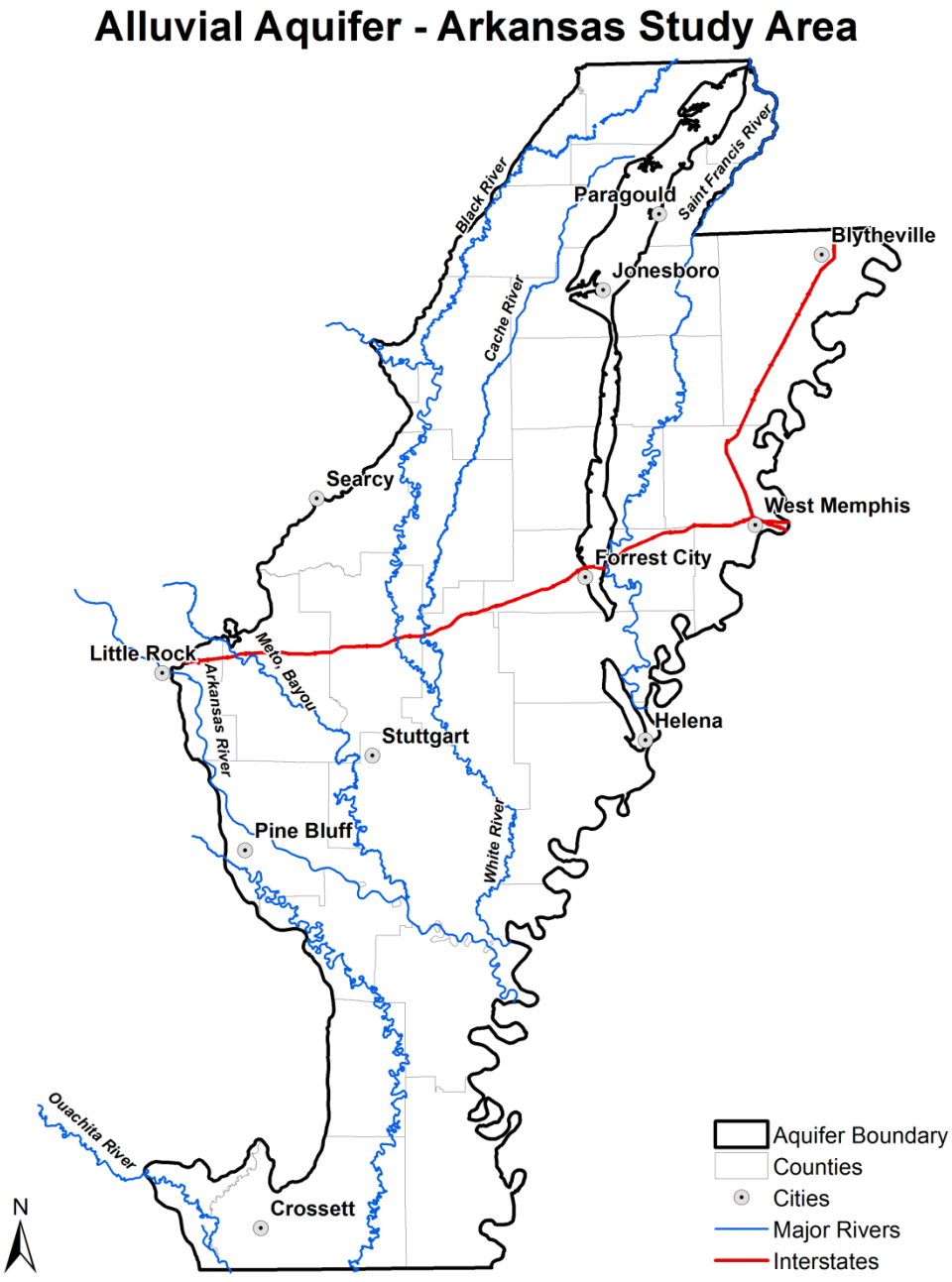

Figure 4. This figure displays the study area relative to various reference points within the study area

3.2. GROUNDWATER FIELD MEASUREMENTS

Groundwater depth field measurements were obtained through the USGS National Water Information System: online interface, which offers groundwater measurements at well sites that

are operated by either of the USGS, ANRC, or the NRCS. This data can be generated in either table or text format and provides data for a number of characteristics associated with each respective measurement site. Spatial Coordinates are represented NAD83 decimal degrees and altitude values are represented in regards to NGVD29. However, the majority of groundwater measurement sites do not record depth values on a daily basis, therefore in this study linear interpolation, with regards to the temporal coverage of known values, is employed as the means of producing groundwater depth values for specified dates. This technique is regularly utilized by USGS for producing groundwater depth plots that demonstrate fluctuations in groundwater levels through time. Data acquisition produced an average 616.2 groundwater measurements in Arkansas for each five-year period. Additionally, groundwater depth samples in neighboring states that are located within a 25-mile buffer of the study area will be utilized during spatial interpolation, however will not factor into the cross validation calculations as this particular case study seeks to determine which spatial interpolation method is the most appropriate for producing groundwater depth estimations in Arkansas.

3.2.1. GROUNDWATER FIELD MEASUREMENTS SPATIAL STATISTICS

The average nearest neighbor tool in the ArcDesktop Spatial Statistics toolbox was employed in this study to calculate spatial coverage statistics associated with the groundwater field measurement sites. The first nearest neighbor values obtained were: 4.105 km in 2015, 3.712 in 2010, 3.975 km in 2005, 4.219 km in 2000 and 4.446 km in 1995. The expected value is relative to the amount of points in relation to the study area size, which grants vital insight into how well the dataset is distributed across the study area. The resulting difference in the expected and the observed nearest neighbor values is a result of clustering of groundwater measurement sites, which is partially caused by large variations from the spatial coverage provided by

measurement sites in Arkansas compared to the coverage in neighboring states. If the average distance is less than the expected average for a certain distribution, it can be concluded that the distribution tends to be clustered. Whereas, if the average distance is greater than the expected average, it can be concluded that the distribution tends to be dispersed. The average nearest neighbor methodology was utilized to calculate the expected mean averages, which were 4.412 km in 2015, 3.848 km in 2010, 3.909 km in 2005, 4 km in 2000, and 4.182 km in 1995. Consequently, it can be concluded that the distribution was considered dispersed in 2015 and 2010, and clustered in 2005, 2000, and 1995.

Table 1. This table displays the average nearest neighbor spatial statistics, which gives valuable insight into a dataset's potential clustering tendencies

Average Nearest Neighbor					
Year	2015	2010	2005	2000	1995
Observed Mean Distance	4.11 km	3.71 km	3.96 km	4.22 km	4.45 km
Expected Mean Distance	4.41km	3.85 km	3.91 km	4 km	4.18 km
Nearest Neighbor Ratio	0.93	0.97	0.99	1.05	1.06
z-score	-3.04	-1.77	-0.43	2.64	2.91
p-value	0.0024	0.076	0.6666	0.0083	0.0036

Table 2. This table displays the average neighbor distance bands. For the distance band number 4 the distance value show represents the average distance to the fourth closest neighbor. This table also gives valuable insight into a dataset's potential clustering tendencies

Average neighbor distance band					
	2015	2010	2005	2000	1995
Distance band 4	9.42 km	8.3 km	8.58 km	8.85 km	9.11 km
Distance band 8	13.66 km	12.03 km	12.46 km	12.9 km	13.27 km
Distance band 16	19.92 km	17.24 km	17.87 km	18.66 km	19.3 km

Additionally, the Global Moran's I Spatial Autocorrelation tool was utilized. Moran's Index values can be interpreted as the following: values near positive 1 indicate that there is a strong spatial autocorrelation; whereas, values near negative 1 indicate strong negative

autocorrelation. Finally, values near 0 indicate a lack of spatial pattern (Rogerson, 2015). The observed Moran's Index values were 0.823 in 2015, 1.053 in 2010, 0.902 in 2005, 0.799 in 2000 and 0.845 in 1995. However, the only significant p-values associated with the Moran's Index values can be found in years 2010 and 1995.

Table 3. This table displays Global Moran's I Spatial Autocorrelation statistics. These statistics give valuable insight regarding a dataset's spatial autocorrelation tendencies.

Spatial Autocorrelation - Global Moran's I					
Year	2015	2010	2005	2000	1995
Moran's Index	0.8228	1.0529	0.9024	0.7991	0.8148
Expected Index	-0.0019	-0.0015	-0.0015	-0.0016	-0.0017
Variance	0.3793	0.2442	0.3134	0.3809	0.0008
z-score	1.339	2.1336	1.6145	1.2973	28.5697
p-value	0.1806	0.0329	0.1064	0.1945	0

3.2.2. GROUNDWATER FIELD MEASUREMENTS DESCRIPTIVE STATISTICS

Table 4. This table displays a variety of spatial statistics related to the Arkansas Groundwater Measurements utilized in this study.

Arkansas Groundwater Measurements					
Year	1995	2000	2005	2010	2015
Number of samples	581	635	665	686	522
Mean	36.49	40.7	43.06	46.29	49.99
Standard deviation	28.36	28.88	31.6	34.18	35.32
Variance	803.98	834.06	998.39	1168.04	1247.23
Coefficient of variation	0.777	0.71	0.734	0.738	0.706
Skewness	1.181	1.145	0.949	0.727	0.67
Kurtosis	0.493	0.494	-0.015	-0.562	-0.666
Q1	15.67	19.42	18.53	18.07	20.05
Median	26.15	30.9	33.02	36.16	39.42
Q3	52.29	57.34	63.35	72.86	77.45
Minimum	2.12	1.93	2.49	0.64	0
Maximum	124.1	138.54	144.99	142.89	148.1

Rstudio was employed for calculating numerous descriptive statistics regarding the groundwater level dataset. The mean depth to the groundwater surface measurement value was calculated as being 36.4927 feet in 1995, while it was calculated as being 49.9915 feet in 2015. The calculated mean value demonstrated consistent increases from each five-year sampling period with an average increase of 3.3737 feet between five-year periods. Similarly, the median value, which was calculated as being 26.1448 in 1995 and 39.4217 in 2015, yielded an increase of 3.3192 feet between five-year periods. Likewise, the calculated standard deviation and variance values yielded steady increases between five-year periods. The coefficient of variation, which is the ratio of the standard deviation relative to the mean, ranged from .706 to .777 between the five-year periods.

The coefficient of skewness value can be described as the measure of the degree of symmetry present within a dataset (Rogerson, 2015, p. 35). The groundwater depth

measurements yielded a skewness value of 1.1806 in 1995 and 0.6697 in 2015, which demonstrates a trend from a positive of left skew towards a more balanced distrbution of groundwater depth measurements (see Figures 4-8). Kurtosis pertains to the shape of a dataset, which is a measure of the degree of tail weight and peak in the distribution of a dataset. The groundwater measurements yielded a kurtosis value of 0.4928 in 1995 to a value of -0.6657 in 2015, which exhibits a trend towards the presence of several extreme values within the dataset.

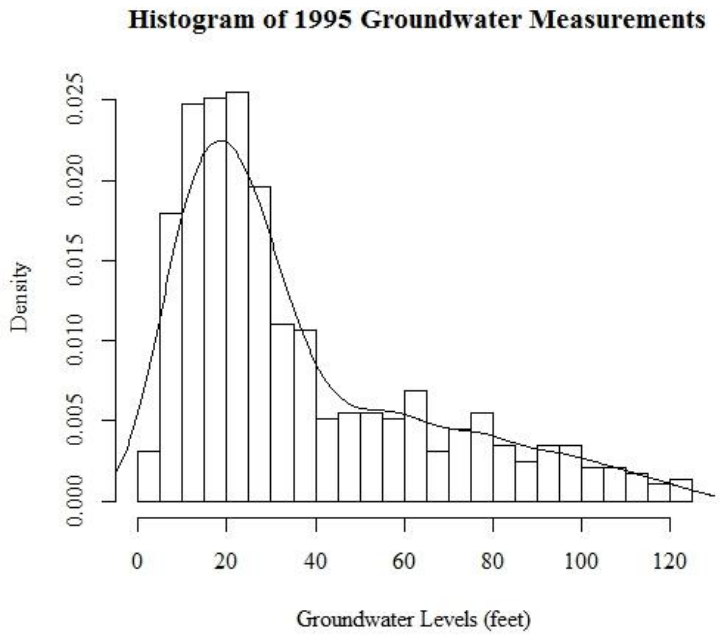

Figure 5. Histogram of 1995 groundwater measurements recorded in the alluvial aquifer in east Arkansas

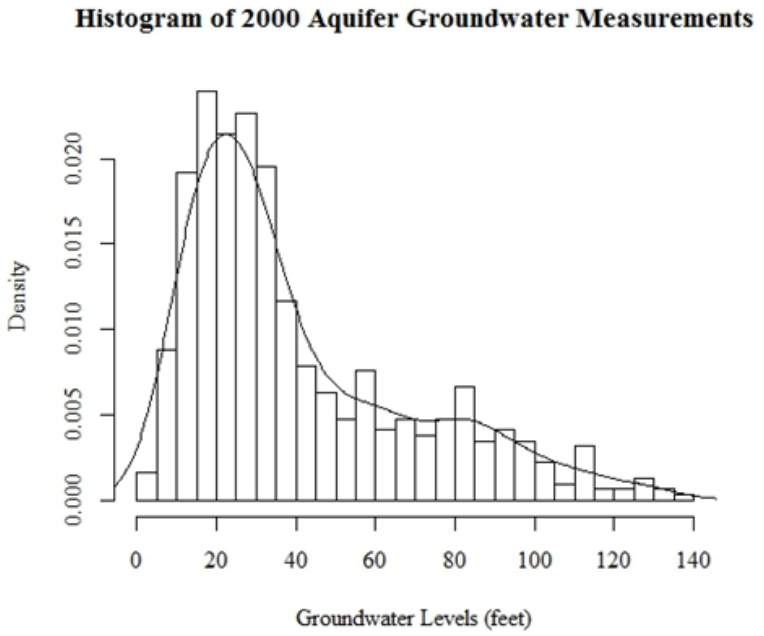

Figure 6. Histogram of 2000 groundwater measurements recorded in the alluvial aquifer in east Arkansas

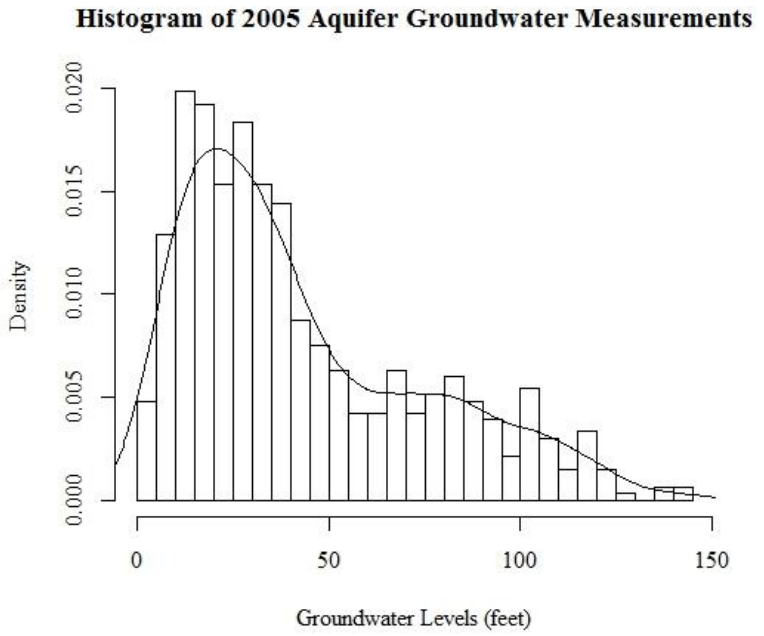

Figure 7. Histogram of 2005 groundwater measurements recorded in the alluvial aquifer in east Arkansas

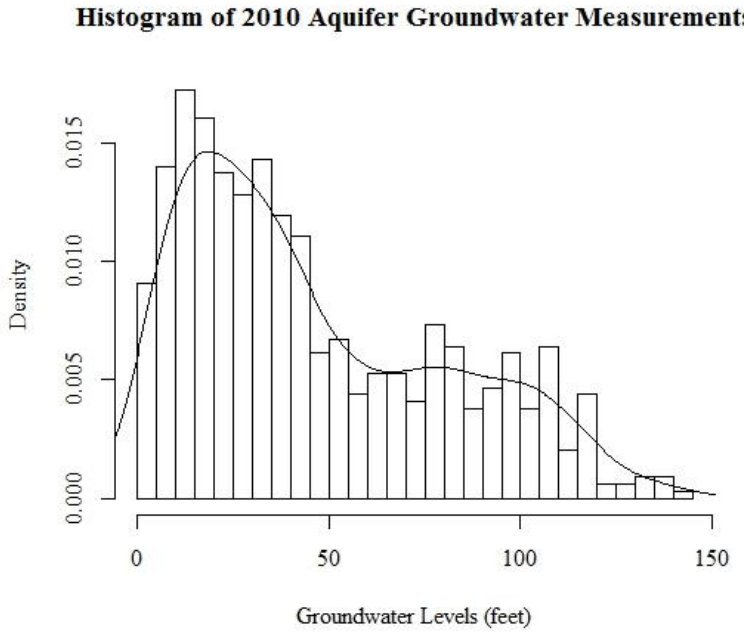

Figure 8. Histogram of 2010 groundwater measurements recorded in the alluvial aquifer in east Arkansas

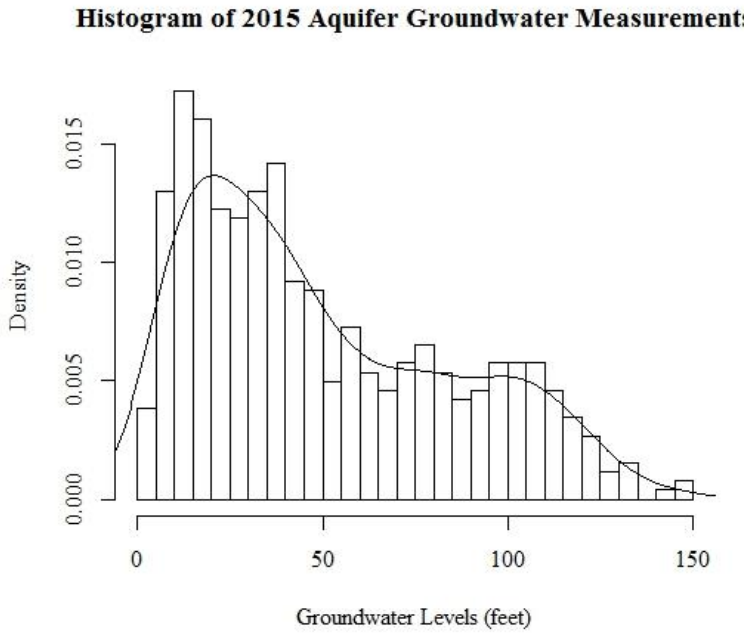

Figure 9. Histogram of 2015 groundwater measurements recorded in the alluvial aquifer in east Arkansas

3.3. SOFTWARE PROGRAMS

3.3.1 ARCGIS DESKTOP 10.X

ArcGIS Desktop, a suite of GIS software developed by Esri, was frequently employed throughout this study. ArcGIS served as the platform where the numerous interpolation methods were carried out. Additionally, ArcGIS provided a valuable means for evaluating and visually exploring data, processing tables of data, and producing maps and figures. Esri's Model Builder, a form of graphical block programming available through the ArcGIS Desktop interface, was employed to construct geoprocessing workflows. Employing ModelBuilder will permit other users to access, modify, or augment the processing workflow constructed in this study.

3.3.2. RSTUDIO

Rstudio refers to an open-source software package, where the R programming language is employed to perform a variety of statistical computations. JJ Allaire founded this statistical language software package in 2008 and it has been commonly employed in the fields of industry, science, and education (RStudio, "Why RStudio?"). Throughout this study, RStudio was employed repeatedly for various purposes related to statistical computation. It provided a constructive means for calculating numerous statistical indicators related to the groundwater measurement datasets as well as the statistical prediction errors related to each spatial interpolation methodology.

3.3.3. MICROSOFT EXCEL

Linear interpolation of Groundwater measurements were calculated using Microsoft Excel. In addition, the groundwater measurements were imported into ArcGIS ModelBuilder in an Excel 97-2003 workbook format. Also, the table to excel tool was utilized in ArcGIS

ModelBuilder to write excel files, which were generally exported into a .csv format to be processed using RStudio software.

3.3.4. ADOBE ILLUSTRATOR

Adobe Illustrator, a graphical design software, was frequently employed for editing the maps and figures produced using ArcGIS software. Adobe Illustrator also provided a constructive means of accessing USGS Aquifer figures and exporting them into a .dwg format to later be georeferenced in ArcGIS.

3.4. STUDY DESIGN

This study seeks to conduct a comparative analysis of the statistical accuracy of seventeen previously discussed spatial interpolation methods. Each method, with the exception of the natural neighbor interpolation method, have numerous adjustable variables that will influence how a particular method will perform estimations. Prior to comparison, these variables will be adjusted accordingly to optimize the statistical accuracy of each particular method. These results will represent the optimal models of each spatial interpolation method. After the optimal models are formulated, the spatial models will be subject to a comparative performance assessment based upon cross-validation and a variety of statistical accuracy indicators.

3.4.1. MODEL PERFORMANCE ASSESSMENT

The statistical accuracy of each model will be assessed utilizing the root means square error (RMSE), mean absolute error (MAE), and coefficient of determination (R^2). RMSE is defined in the ESRI GIS dictionary as the difference between known locations and locations that have been digitized or interpolated. RMS error can be calculated by taking the square root of the differences among known and unknown points, obtaining the sum of these values, dividing it by

the total number of test points, and by taking the square root of that resulted value (RMS error, n.d.). The coefficient of determination, also known as R-squared, is defined by the ESRI GIS Dictionary as a statistic calculated by the regression equation to measure the performance of the model. The values of the coefficient of determination range from 0 to 100 percent. (R-squared, n.d.). The mean absolute error is a standard metric utilized to measure the expected error of the system (Tamayo, 2012).

3.4.2. GIGAWATT

All ArcGIS ModelBuilder workflows in this particular case study were carried out utilizing a server-based GIS tool referred to as *Gigawatt*. According to Tullis's unpublished manuscript, *Gigawatt* promotes a highly collaborative environment by allowing ModelBuilder workflows to be easily exchanged between a designated group of individuals. Additionally, by providing the ability to re-execute a workflow, *Gigawatt* allows for detailed and comprehensive provenance information. In this situation, provenance refers to a record of the specific geoprocesses from which any resulting geospatial datasets are derived (Tullis et al., 2015, p. 402).

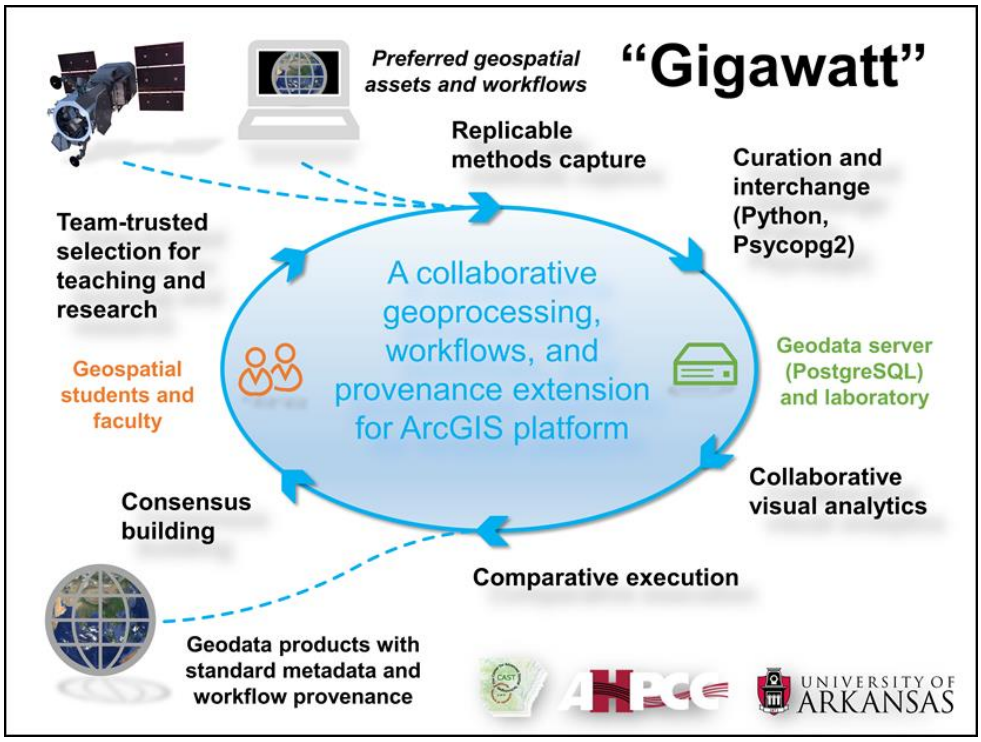

Figure 10. This figure demonstrates the general concept of the Gigawatt tool (Tullis, unpublished) Reprinted with permission.

4. RESULTS

4.1. 1995 INTERPOLATED SURFACES

Multiquadric spline produced the estimated surface with the highest statistical accuracy in 1995. The average prediction errors yielded were a RMSE of 8.9259 and MAE of 6.0115, while generating an average coefficient of determination value of 0.9008. Ordinary kriging produced the surface with the second highest statistical accuracy, yielding an average RMSE of 9.0127, a MAE of 6.2209, and coefficient of determination value of 0.8989. Kernel interpolation with barriers produced the surface with the third highest statistical accuracy, yielding an average RMSE of 9.186, a MAE of 6.3058, and coefficient of determination value of 0.8959.

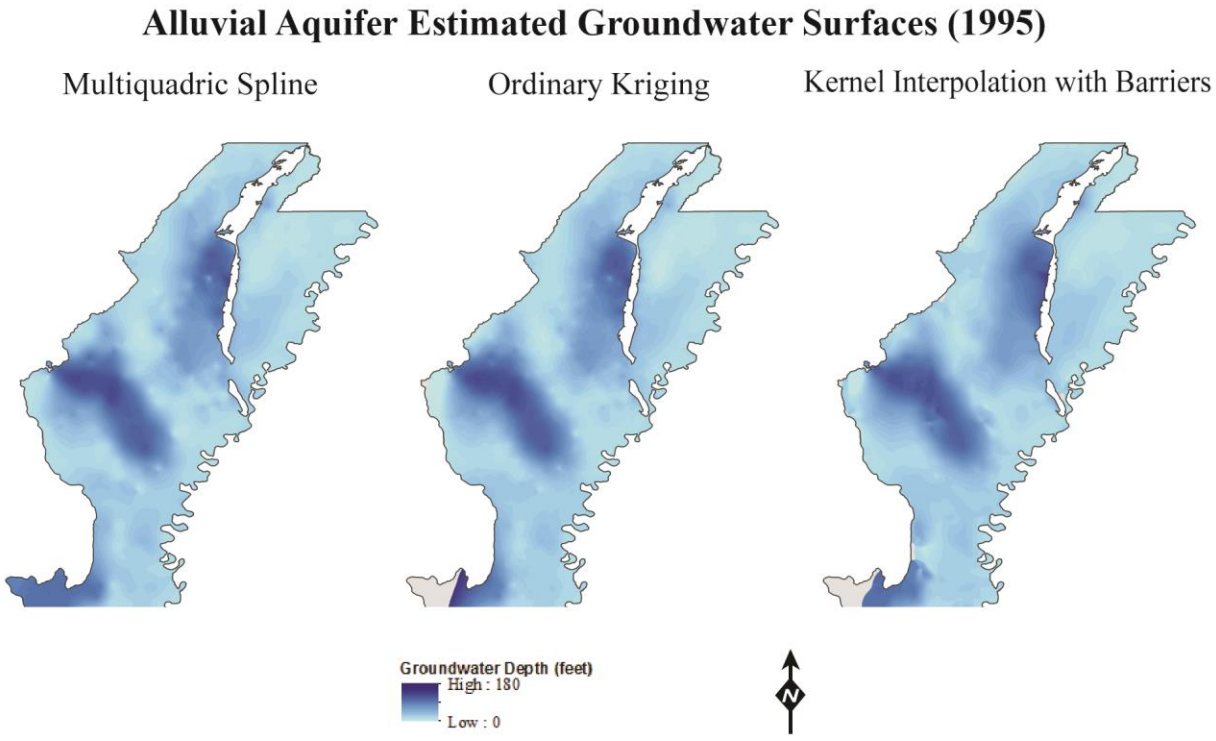

Figure 11. This figure displays the estimated groundwater surfaces generated from multiquadric spline, ordinary kriging, and kernel interpolation with barriers interpolation methods in 1995

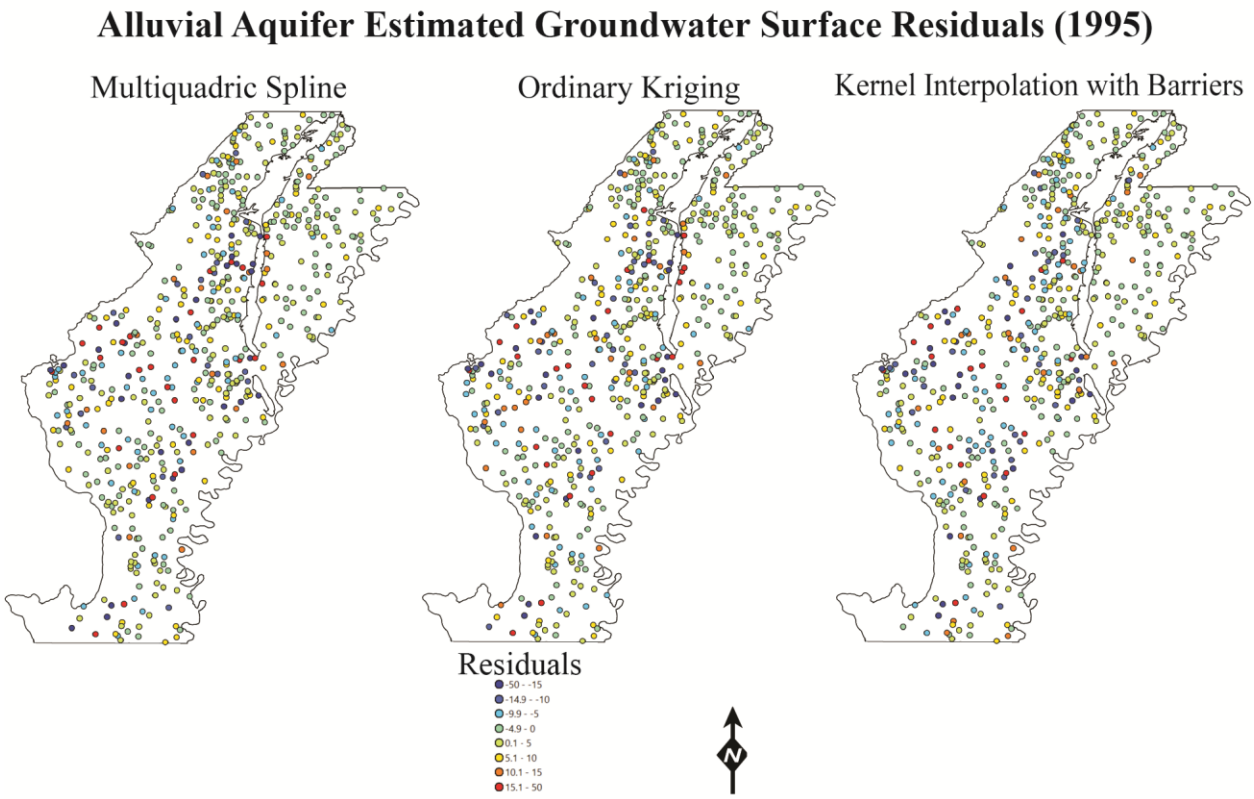

Figure 12. This figure displays the residuals spatially yielded by multiquadric spline, ordinary kriging, and kernel interpolation with barriers interpolation methods in 1995

Table 5. 1995 Leave-out One Cross Validation

1995 Leave-out One Cross Validation			
Spatial Interpolation Model	RMSE	MAE	R^2
Ordinary Kriging	8.8481	6.0597	0.9025
Universal Kriging	9.7871	6.8271	0.8816
Empirical Bayesian Kriging	9.1068	6.0331	0.8967
Simple Kriging	9.4406	6.4895	0.8895
IDW	9.5430	6.4564	0.8874
Tension Spline	9.0383	6.0301	0.8984
Regularized Spline	9.2495	6.2866	0.8952
Local Polynomial Interpolation	9.1539	6.1694	0.8971
Global Polynomial Interpolation	17.3981	11.7069	0.6380
Diffusion Interpolation with Barriers	10.7890	7.6488	0.8616
Kernel Interpolation with Barriers	9.0460	6.2120	0.8992
Multiquadric Spline	8.7978	5.8675	0.9036
Inverse Multiquadric Spline	9.9675	6.7572	0.8762
Thin Plate Spline	9.4205	6.3593	0.8906

Table 6. 1995 k-Fold Cross Validation

1995 k-Fold Cross Validation			
Spatial Interpolation Model	RMSE	MAE	R^2
Ordinary Kriging	9.1772	6.3822	0.8953
Universal Kriging	9.2627	6.5816	0.8938
Empirical Bayesian Kriging	9.7451	6.5277	0.8820
Simple Kriging	9.8026	6.8598	0.8811
IDW	10.0595	6.9029	0.8748
Tension Spline	9.3480	6.3516	0.8916
Regularized Spline	9.6486	6.6474	0.8865
Local Polynomial Interpolation	9.6109	6.5702	0.8860
Global Polynomial Interpolation	18.4309	11.8181	0.6050
Nearest Neighbor	9.5349	N/A	0.8884
IDW with Barriers	9.8932	6.7065	0.8784
Spline with Barriers	9.2872	6.2004	0.8935
Diffusion Interpolation with Barriers	11.0902	7.8666	0.8529
Kernel Interpolation with Barriers	9.3259	6.3996	0.8927
Multiquadric Spline	9.0541	6.1555	0.8981
Inverse Multiquadric Spline	10.2364	7.0021	0.8697
Thin Plate Spline	9.9322	6.7312	0.8935

4.1.1. 1995 CROWLEY'S RIDGE BUFFER

For the Crowley's Ridge Scenario, the kernel interpolation with barriers produced the estimated surface with the highest statistical accuracy in 1995. The average prediction errors yielded were a RMSE of 8.074 and MAE of 5.358, while generating an average coefficient of determination value of 0.922. Spline with barriers produced the surface with the second highest statistical accuracy, yielding a k-Fold cross validation RMSE of 8.556, a MAE of 5.542, and coefficient of determination value of 0.9133. IDW with barriers produced the surface with the third highest statistical accuracy, yielding a k-Fold cross validation RMSE of 8.691, a MAE of 5.898, and coefficient of determination value of 0.9101.

Table 7. 1995 k-Fold Cross Validation Crowley's Ridge

1995 k-Fold Cross Validation			
Spatial Interpolation Model	RMSE	MAE	R^2
Ordinary Kriging	9.2612	6.3059	0.8977
Universal Kriging	9.9553	6.9857	0.8815
Empirical Bayesian Kriging	9.9825	6.5687	0.8809
Simple Kriging	10.1613	6.8463	0.8777
IDW	9.6156	6.4680	0.8897
Tension Spline	9.2651	6.0270	0.8973
Regularized Spline	9.3355	6.1482	0.8964
Local Polynomial Interpolation	9.6615	6.3727	0.8893
Global Polynomial Interpolation	14.7014	11.0877	0.7415
Nearest Neighbor	9.6627	6.3929	0.8887
IDW with Barriers	8.6913	5.8980	0.9101
Spline with Barriers	8.5561	5.5419	0.9133
Diffusion Interpolation with Barriers	9.4176	6.7852	0.8970
Kernel Interpolation with Barriers	8.1290	5.4780	0.9210
Multiquadric Spline	9.1771	6.0286	0.8993
Inverse Multiquadric Spline	9.8811	6.4154	0.8836
Thin Plate Spline	9.6413	6.4362	0.9133

Table 8. 1995 Leave-out One Cross Validation Crowley's Ridge

1995 Leave-out One Cross Validation			
Spatial Interpolation Model	RMSE	MAE	R^2
Ordinary Kriging	9.0297	5.9922	0.9026
Universal Kriging	9.9884	6.9451	0.8810
Empirical Bayesian Kriging	9.5996	5.9434	0.8901
Simple Kriging	9.8644	6.4464	0.8844
IDW	9.2286	6.0566	0.8985
Tension Spline	8.9795	5.6683	0.9036
Regularized Spline	9.0407	5.7850	0.9026
Local Polynomial Interpolation	9.4015	6.0297	0.8953
Global Polynomial Interpolation	14.6574	11.0259	0.7431
Diffusion Interpolation with Barriers	9.2722	6.5926	0.9005
Kernel Interpolation with Barriers	8.0193	5.2377	0.9231
Multiquadric Spline	8.8873	5.6359	0.9055
Inverse Multiquadric Spline	9.6936	6.3263	0.8881
Thin Plate Spline	9.1990	6.0124	0.8994

4.2. 2000 INTERPOLATED SURFACES

Ordinary kriging produced the estimated surface with the highest statistical accuracy in 2000. The average prediction errors yielded were a RMSE of 9.3621 and MAE of 6.2611, while generating an average coefficient of determination value of 0.8949. Simple kriging produced the surface with the second highest statistical accuracy, yielding an average RMSE of 9.3752, a MAE of 6.244, and coefficient of determination value of 0.8946. Local polynomial interpolation produced the surface with the third highest statistical accuracy, yielding an average RMSE of 9.4284, a MAE of 6.3292, and coefficient of determination value of 0.8932.

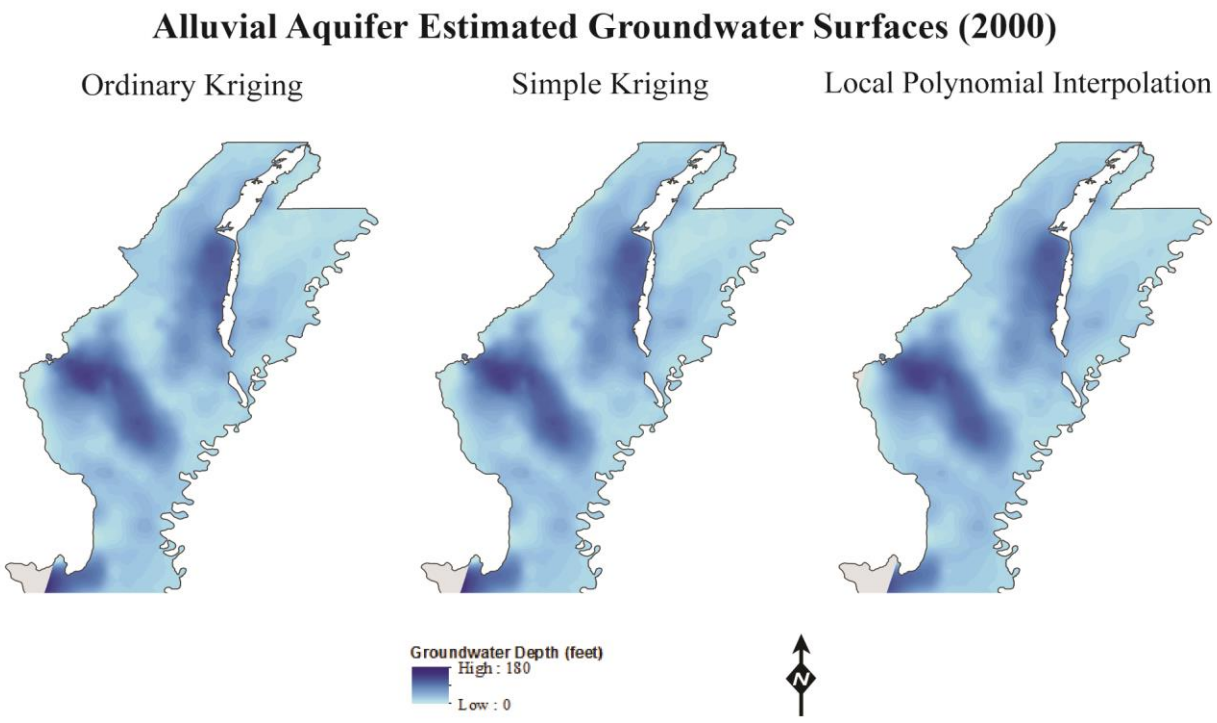

Figure 13. This figure displays the estimated groundwater surfaces generated from ordinary kriging, simple kriging, and local polynomial interpolation methods in 2000

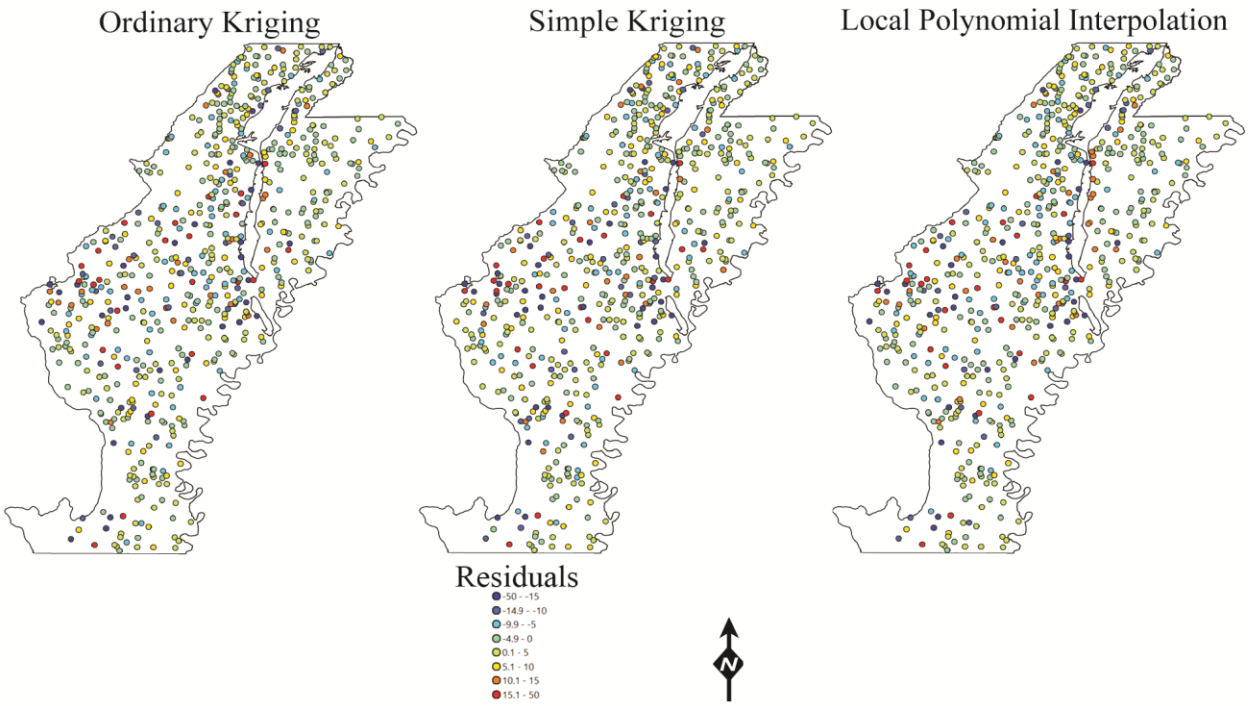

Figure 14. This figure displays the residuals spatially yielded by ordinary kriging, simple kriging and local polynomial interpolation methods in 2000

Table 9. 2000 Leave-out One Cross Validation

2000 Leave-out One Cross Validation			
Spatial Interpolation Model	RMSE	MAE	R^2
Ordinary Kriging	9.0834	6.1947	0.9010
Universal Kriging	10.0958	6.8240	0.8782
Empirical Bayesian Kriging	9.2834	6.1963	0.8967
Simple Kriging	9.1055	6.1727	0.9005
IDW	9.5093	6.4575	0.8933
Tension Spline	9.5236	6.2459	0.8913
Regularized Spline	9.8262	6.4548	0.8843
Local Polynomial Interpolation	9.1212	6.2524	0.9001
Global Polynomial Interpolation	16.2569	11.9239	0.6854
Diffusion Interpolation with Barriers	10.0296	7.1156	0.8817
Kernel Interpolation with Barriers	10.0117	7.1195	0.8875
Multiquadric Spline	9.2434	6.0580	0.8977
Inverse Multiquadric Spline	9.9725	6.5947	0.8813
Thin Plate Spline	9.6720	6.3362	0.8882

Table 10. 2000 k-Fold Cross Validation

2000 k-Fold Cross Validation			
Spatial Interpolation Model	RMSE	MAE	R^2
Ordinary Kriging	9.6407	6.3275	0.8888
Universal Kriging	10.8247	7.0524	0.8609
Empirical Bayesian Kriging	9.6470	6.3526	0.8884
Simple Kriging	9.6449	6.3152	0.8886
IDW	9.9640	6.6295	0.8820
Tension Spline	9.9338	6.3837	0.8823
Regularized Spline	9.9608	6.4527	0.8816
Local Polynomial Interpolation	9.7356	6.4059	0.8863
Global Polynomial Interpolation	16.5131	11.9959	0.6761
Nearest Neighbor	9.8106	N/A	0.8848
IDW with Barriers	10.1812	6.5962	0.8757
Spline with Barriers	9.6391	6.1680	0.8898
Diffusion Interpolation with Barriers	10.3144	7.0914	0.8739
Kernel Interpolation with Barriers	9.6787	6.4552	0.8892
Multiquadric Spline	9.6602	6.2261	0.8881
Inverse Multiquadric Spline	10.0887	6.5730	0.8791
Thin Plate Spline	10.2353	6.4957	0.8898

4.2.1. 2000 CROWLEY'S RIDGE BUFFER

For the Crowley's Ridge Scenario, the spline with barriers interpolation method produced the estimated surface with the highest statistical accuracy in 2000. The average prediction errors yielded were a RMSE of 7.892 and MAE of 5.215, while generating an average coefficient of determination value of 0.925. IDW with barriers produced the surface with the second highest statistical accuracy, yielding a k-Fold cross validation RMSE of 8.018, a MAE of 5.53, and coefficient of determination value of 0.922. The kernel interpolation with barriers method produced the surface with the third highest statistical accuracy, yielding a k-Fold cross validation RMSE of 8.127, a MAE of 5.9, and coefficient of determination value of 0.921.

Table 11. 2000 Leave-out One Cross Validation Crowley's Ridge

2000 Leave-out One Cross Validation			
Spatial Interpolation Model	RMSE	MAE	R^2
Ordinary Kriging	8.6628	6.1336	0.9082
Universal Kriging	10.0872	6.7736	0.8756
Empirical Bayesian Kriging	8.8508	5.6064	0.9043
Simple Kriging	8.6328	6.0868	0.9090
IDW	8.6629	5.9210	0.9107
Tension Spline	8.3768	5.6298	0.9142
Regularized Spline	8.5584	5.7928	0.9107
Local Polynomial Interpolation	8.9148	6.3760	0.9031
Global Polynomial Interpolation	15.0379	11.8071	0.7236
Diffusion Interpolation with Barriers	9.0857	6.6887	0.9012
Kernel Interpolation with Barriers	8.3987	6.1958	0.9164
Multiquadric Spline	8.2974	5.4582	0.9166
Inverse Multiquadric Spline	8.7184	5.9318	0.9077
Thin Plate Spline	8.4944	5.7176	0.9118

Table 12. 2000 k-Fold Cross Validation Crowley's Ridge

2000 k-Fold Cross Validation			
Spatial Interpolation Model	RMSE	MAE	R^2
Ordinary Kriging	8.8670	6.1686	0.9038
Universal Kriging	10.6937	7.0923	0.8606
Empirical Bayesian Kriging	9.0853	5.8213	0.8991
Simple Kriging	8.8335	6.1624	0.9046
IDW	8.7751	6.0344	0.9080
Tension Spline	8.6433	5.7537	0.9086
Regularized Spline	8.5015	5.7600	0.9116
Local Polynomial Interpolation	9.0445	6.4161	0.9003
Global Polynomial Interpolation	15.0389	11.7708	0.7235
Nearest Neighbor	8.8922	5.9292	0.9043
IDW with Barriers	8.0184	5.5300	0.9217
Spline with Barriers	7.8923	5.2153	0.9252
Diffusion Interpolation with Barriers	8.9097	6.6129	0.9047
Kernel Interpolation with Barriers	7.8548	5.6045	0.9258
Multiquadric Spline	8.6886	5.7522	0.9084
Inverse Multiquadric Spline	8.5894	5.8245	0.9099
Thin Plate Spline	8.7871	5.8127	0.9252

4.3. 2005 INTERPOLATED SURFACES

Local polynomial interpolation produced the estimated surface with the highest statistical accuracy in 2005. The average prediction errors yielded were a RMSE of 10.2167 and MAE of 6.8081, while generating an average coefficient of determination value of 0.8948. Empirical Bayesian kriging produced the surface with the second highest statistical accuracy, yielding an average RMSE of 10.2289, a MAE of 6.807, and coefficient of determination value of 0.8946. Ordinary kriging produced the surface with the third highest statistical accuracy, yielding an average RMSE of 10.26215, a MAE of 6.8589, and coefficient of determination value of 0.8939.

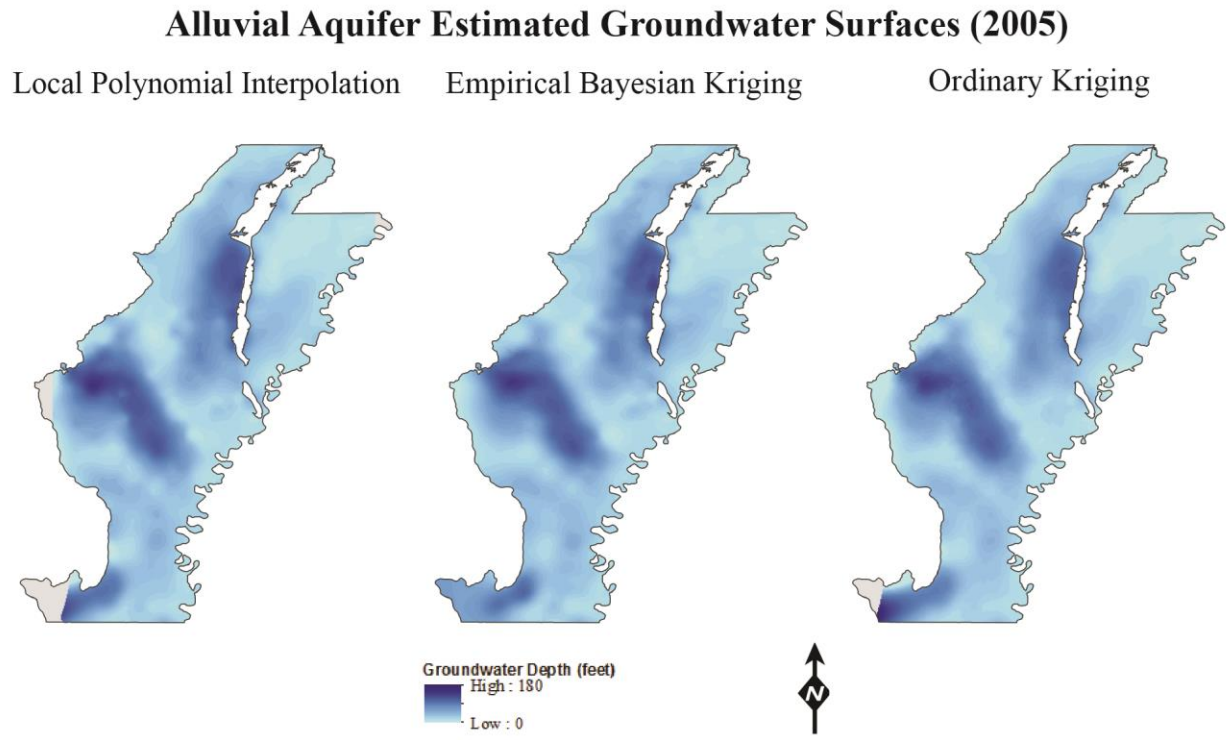

Figure 15. This figure displays the estimated groundwater surfaces generated from local polynomial interpolation, empirical Bayesian kriging, and ordinary kriging interpolation methods in 2005

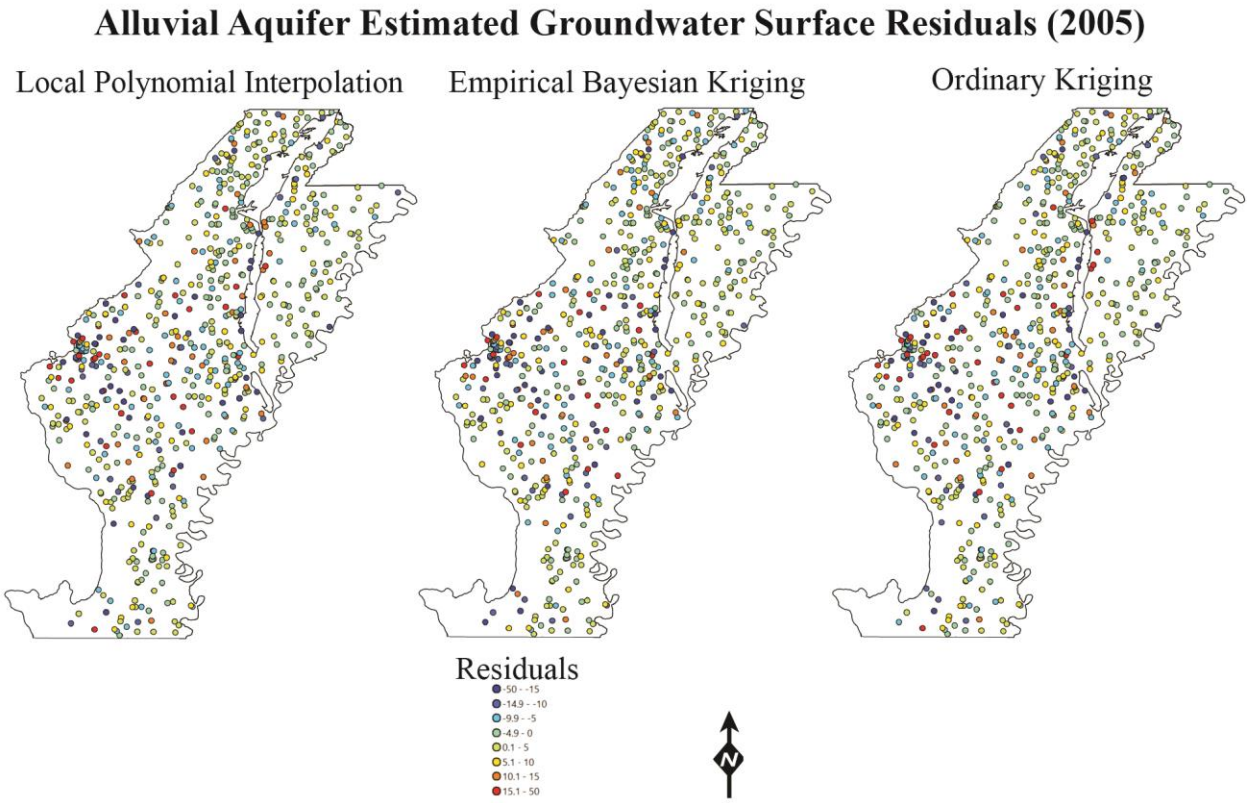

Figure 16. This figure displays the residuals spatially yielded by local polynomial interpolation, empirical Bayesian kriging and ordinary kriging interpolation methods in 2005

Table 13. 2005 Leave-out One Cross Validation

2005 Leave-out One Cross Validation			
Spatial Interpolation Model	RMSE	MAE	R^2
Ordinary Kriging	10.1815	6.9123	0.8960
Universal Kriging	11.2039	7.8171	0.8741
Empirical Bayesian Kriging	10.1188	6.8148	0.8975
Simple Kriging	10.2441	6.9260	0.8947
IDW	10.6978	7.1188	0.8860
Tension Spline	10.7535	6.9213	0.8840
Regularized Spline	11.2657	7.2253	0.8732
Local Polynomial Interpolation	10.2484	6.8819	0.8946
Global Polynomial Interpolation	19.7721	13.1146	0.6232
Diffusion Interpolation with Barriers	11.3896	7.8381	0.8725
Kernel Interpolation with Barriers	10.3472	7.0499	0.8944
Multiquadric Spline	10.5593	6.9130	0.8882
Inverse Multiquadric Spline	11.1745	7.0857	0.8754
Thin Plate Spline	11.1961	7.0845	0.8757

Table 14. 2005 k-Fold Cross Validation

2005 k-Fold Cross Validation			
Spatial Interpolation Model	RMSE	MAE	R^2
Ordinary Kriging	10.3428	6.8055	0.8917
Universal Kriging	11.6030	7.9494	0.8639
Empirical Bayesian Kriging	10.3390	6.7993	0.8917
Simple Kriging	10.4177	6.8479	0.8900
IDW	10.5280	6.8204	0.8882
Tension Spline	10.2662	6.5592	0.8934
Regularized Spline	10.6696	6.6636	0.8848
Local Polynomial Interpolation	10.1850	6.7343	0.8949
Global Polynomial Interpolation	20.3110	13.0694	0.6057
Nearest Neighbor	10.7238	N/A	0.8835
IDW with Barriers	10.6711	6.9557	0.8847
Spline with Barriers	10.4159	6.5312	0.8908
Diffusion Interpolation with Barriers	11.5263	7.8572	0.8676
Kernel Interpolation with Barriers	10.5187	6.9918	0.8888
Multiquadric Spline	10.4004	6.6768	0.8905
Inverse Multiquadric Spline	10.6870	6.6339	0.8849
Thin Plate Spline	10.3983	6.6913	0.8908

4.3.1 2005 CROWLEY'S RIDGE BUFFER

For the Crowley's Ridge Scenario, the spline with barriers interpolation method produced the estimated surface with the highest statistical accuracy in 2005. The k-Fold prediction errors yielded were a RMSE of 7.98 and MAE of 5.468, while generating an average coefficient of determination value of 0.934. The multiquadric spline method produced the surface with the second highest statistical accuracy, yielding a k-Fold cross validation RMSE of 8.28, a MAE of 5.753 and coefficient of determination value of 0.929. The thin plate spline method produced the surface with the third highest statistical accuracy, yielding an average RMSE of 8.499, a MAE of 5.756, and coefficient of determination value of 0.929.

Table 15. 2005 k-Fold Cross Validation Crowley's Ridge

2005 k-Fold Cross Validation			
Spatial Interpolation Model	RMSE	MAE	R^2
Ordinary Kriging	9.2696	6.4286	0.9113
Universal Kriging	11.7194	8.3439	0.8590
Empirical Bayesian Kriging	8.7220	6.1728	0.9214
Simple Kriging	9.3188	6.5432	0.9107
IDW	9.3036	6.4583	0.9123
Tension Spline	8.5132	5.9498	0.9251
Regularized Spline	8.6221	6.0358	0.9232
Local Polynomial Interpolation	8.8267	6.3618	0.9196
Global Polynomial Interpolation	15.5889	11.8735	0.7488
Nearest Neighbor	8.6056	6.1530	0.9247
IDW with Barriers	8.6663	6.1059	0.9225
Spline with Barriers	7.9802	5.4683	0.9343
Diffusion Interpolation with Barriers	9.4520	6.7674	0.9090
Kernel Interpolation with Barriers	8.3443	5.9648	0.9282
Multiquadric Spline	8.5804	6.0369	0.9247
Inverse Multiquadric Spline	8.5428	5.9460	0.9246
Thin Plate Spline	8.6543	6.2198	0.9343

Table 16. 2005 Leave-out One Cross Validation Crowley's Ridge

2005 Leave-out One Cross Validation			
Spatial Interpolation Model	RMSE	MAE	R^2
Ordinary Kriging	9.26955	6.42858	0.91132
Universal Kriging	11.7194	8.34386	0.85898
Empirical Bayesian Kriging	8.72203	6.17281	0.92144
Simple Kriging	9.31878	6.54318	0.91071
IDW	9.30364	6.45828	0.91229
Tension Spline	8.51324	5.94976	0.92512
Regularized Spline	8.6221	6.03577	0.92319
Local Polynomial Interpolation	8.82668	6.36185	0.91958
Global Polynomial Interpolation	15.5889	11.8735	0.74881
Diffusion Interpolation with Barriers	9.45204	6.7674	0.90899
Kernel Interpolation with Barriers	8.34433	5.96477	0.92817
Multiquadric Spline	8.58039	6.03688	0.92468
Inverse Multiquadric Spline	8.54285	5.94604	0.9246
Thin Plate Spline	8.65431	6.21981	0.923

4.4. 2010 INTERPOLATED SURFACES

Empirical Bayesian kriging produced the estimated surface with the highest statistical accuracy in 2010. The average prediction errors yielded were a RMSE of 10.9125 and MAE of 7.1533, while generating an average coefficient of determination value of 0.8978. Kernel interpolation with barriers produced the surface with the second highest statistical accuracy, yielding an average RMSE of 11.1554, a MAE of 7.6045, and coefficient of determination value of 0.8952. Multiquadric spline produced the surface with the third highest statistical accuracy, yielding an average RMSE of 11.2378, a MAE of 7.1523, and coefficient of determination value of 0.8917.

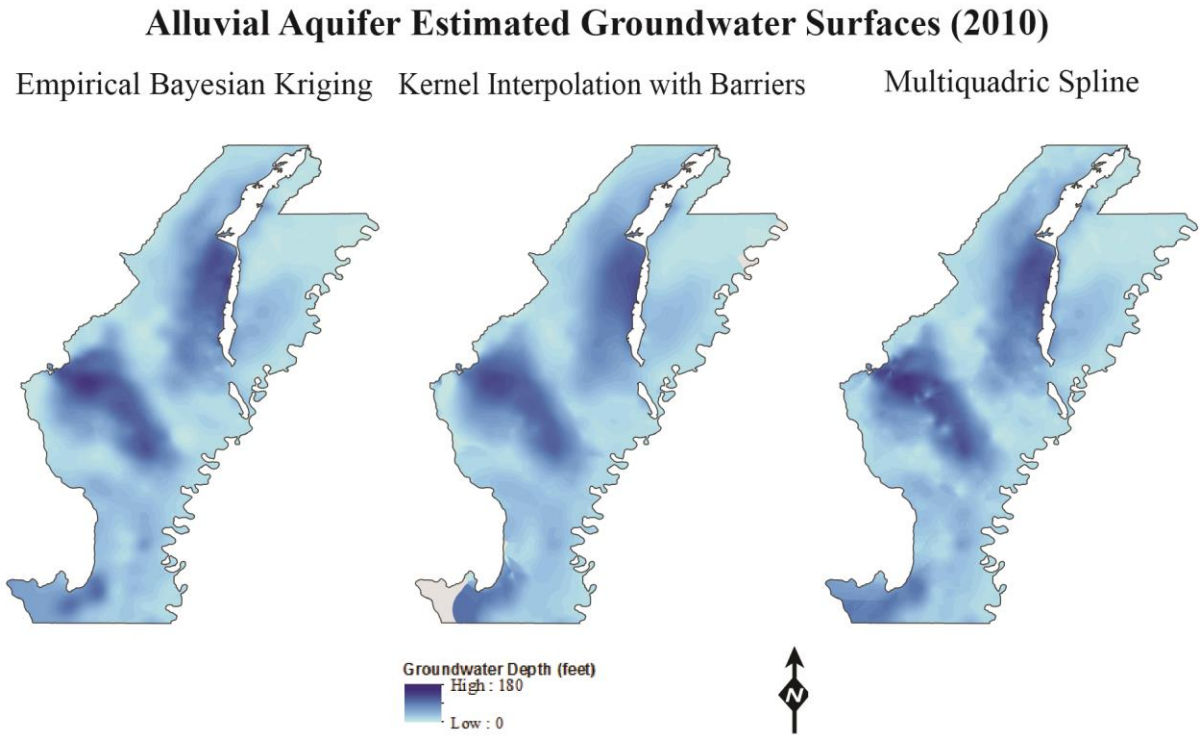

Figure 17. This figure displays the estimated groundwater surfaces generated from empirical Bayesian kriging, kernel interpolation with barriers, and multiquadric spline interpolation methods in 2010

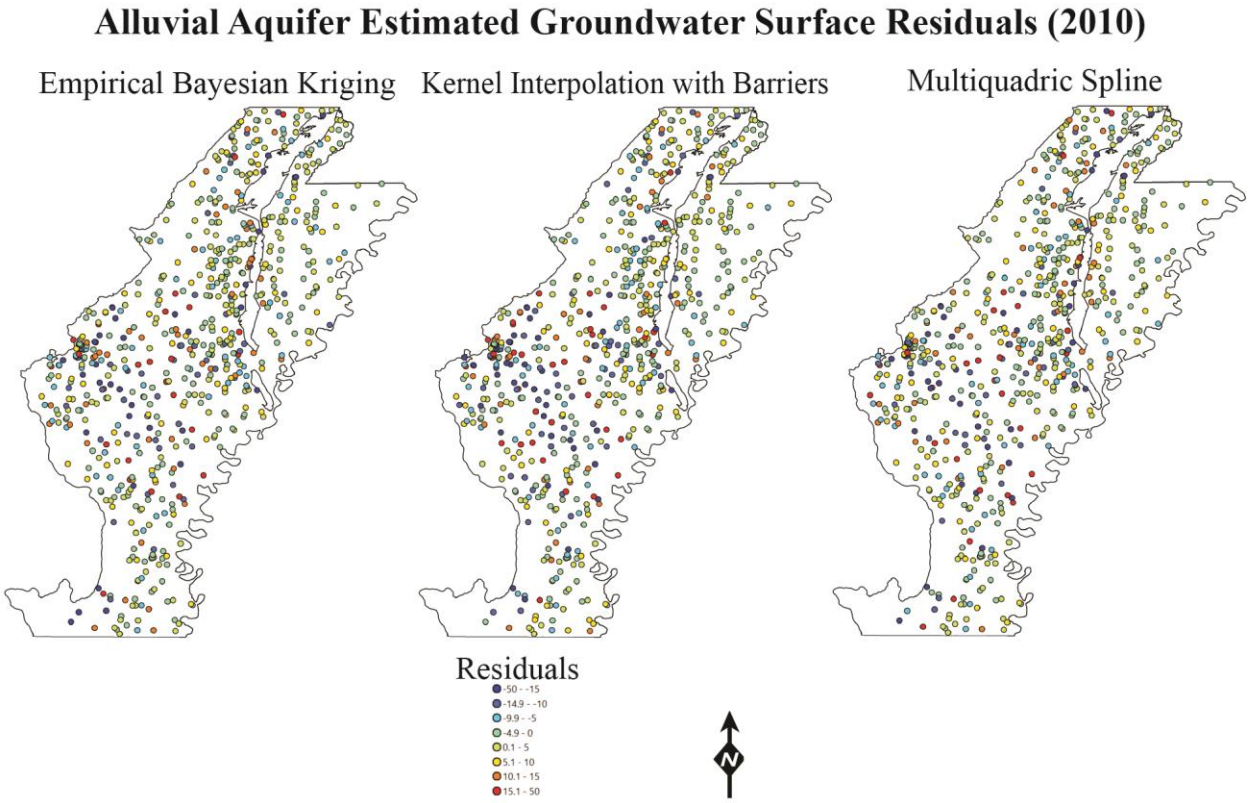

Figure 18. This figure displays the residuals spatially yielded by empirical Bayesian kriging, kernel interpolation with barriers, and multiquadric spline interpolation methods in 2010

Table 17. 2010 Leave-out One Cross Validation

2010 Leave-out One Cross Validation			
Spatial Interpolation Model	RMSE	MAE	R^2
Ordinary Kriging	10.9814	7.5408	0.8966
Universal Kriging	11.4772	7.9320	0.8870
Empirical Bayesian Kriging	10.5432	6.8975	0.9047
Simple Kriging	11.1170	7.5727	0.8941
IDW	11.1813	7.3238	0.8934
Tension Spline	11.3335	7.2022	0.8901
Regularized Spline	11.4713	7.3553	0.8873
Local Polynomial Interpolation	11.0592	7.5386	0.8955
Global Polynomial Interpolation	18.2769	13.6618	0.7157
Diffusion Interpolation with Barriers	12.3577	8.5214	0.8711
Kernel Interpolation with Barriers	10.8637	7.4967	0.9011
Multiquadric Spline	11.0245	7.0516	0.8957
Inverse Multiquadric Spline	11.6790	7.4263	0.8837
Thin Plate Spline	11.5376	7.4325	0.8869

Table 18. 2010 k-Fold Cross Validation

2010 k-Fold Cross Validation			
Spatial Interpolation Model	RMSE	MAE	R^2
Ordinary Kriging	11.9066	7.9952	0.8785
Universal Kriging	12.7874	8.3998	0.8603
Empirical Bayesian Kriging	11.2818	7.4090	0.8909
Simple Kriging	12.1189	8.1176	0.8742
IDW	11.6618	7.6614	0.8841
Tension Spline	11.6546	7.3748	0.8839
Regularized Spline	16.2548	8.0607	0.7951
Local Polynomial Interpolation	11.4691	7.6481	0.8873
Global Polynomial Interpolation	20.2943	14.0820	0.6582
Nearest Neighbor	11.6378	7.3770	0.8840
IDW with Barriers	12.0499	7.7722	0.8758
Spline with Barriers	11.9300	7.5104	0.8794
Diffusion Interpolation with Barriers	12.7512	8.6594	0.8624
Kernel Interpolation with Barriers	11.4471	7.7122	0.8893
Multiquadric Spline	11.4510	7.2530	0.8876
Inverse Multiquadric Spline	11.7264	7.4884	0.8823
Thin Plate Spline	12.5815	7.6943	0.8794

4.4.1. 2010 CROWLEY'S RIDGE BUFFER

For the Crowley's Ridge Scenario, the spline with barriers method produced the estimated surface with the highest statistical accuracy in 2010. The average prediction errors yielded were a RMSE of 9.0574, and MAE of 5.911, while generating an average coefficient of determination value of 0.934. The kernel interpolation with barriers produced the surface with the second highest statistical accuracy, yielding an average RMSE of 8.683, a MAE of 5.942, and coefficient of determination value of 0.939. The empirical Bayesian kriging method produced the surface with the third highest statistical accuracy, yielding an average RMSE of 9.525, a MAE of 6.153, and coefficient of determination value of 0.926.

Table 19. 2010 Leave-out One Cross Validation Crowley's Ridge

2010 Leave-out One Cross Validation			
Spatial Interpolation Model	RMSE	MAE	R^2
Ordinary Kriging	10.3482	7.2254	0.9129
Universal Kriging	11.1248	7.8882	0.8993
Empirical Bayesian Kriging	9.3500	5.9661	0.9287
Simple Kriging	10.2083	6.9056	0.9153
IDW	9.3085	6.1820	0.9297
Tension Spline	9.7582	6.2745	0.9226
Regularized Spline	9.8910	6.4394	0.9206
Local Polynomial Interpolation	10.4172	7.1225	0.9122
Global Polynomial Interpolation	15.7265	11.8848	0.7988
Diffusion Interpolation with Barriers	9.8512	6.7495	0.9212
Kernel Interpolation with Barriers	8.6529	5.9299	0.9390
Multiquadric Spline	9.5011	6.1658	0.9264
Inverse Multiquadric Spline	10.1191	6.5878	0.9176
Thin Plate Spline	10.0626	6.6195	0.9180

Table 20. 2010 k-Fold Cross Validation Crowley's Ridge

2010 k-Fold Cross Validation			
Spatial Interpolation Model	RMSE	MAE	R^2
Ordinary Kriging	10.5217	7.5298	0.9101
Universal Kriging	11.4601	8.1226	0.8931
Empirical Bayesian Kriging	9.7002	6.3399	0.9235
Simple Kriging	10.6325	7.4203	0.9084
IDW	9.6197	6.4505	0.9249
Tension Spline	9.6958	6.2414	0.9235
Regularized Spline	9.8730	6.3791	0.9208
Local Polynomial Interpolation	10.2378	7.0916	0.9147
Global Polynomial Interpolation	15.7284	11.9151	0.7986
Nearest Neighbor	9.5911	6.2192	0.9251
IDW with Barriers	9.6243	6.3767	0.9246
Spline with Barriers	9.0574	5.9116	0.9345
Diffusion Interpolation with Barriers	9.8947	6.7947	0.9204
Kernel Interpolation with Barriers	8.7128	5.9534	0.9382
Multiquadric Spline	9.5839	6.2270	0.9251
Inverse Multiquadric Spline	9.6910	6.1975	0.9235
Thin Plate Spline	10.1628	6.5350	0.9345

4.5. 2015 INTERPOLATED SURFACES

Simple kriging produced the estimated surface with the highest statistical accuracy in 2015. The average prediction errors yielded were a RMSE of 12.4984 and MAE of 7.9941, while generating an average coefficient of determination value of 0.8751. Ordinary kriging produced the surface with the second highest statistical accuracy, yielding an average RMSE of 12.5098, a MAE of 8.1027, and coefficient of determination value of 0.8749. Local polynomial interpolation produced the surface with the third highest statistical accuracy, yielding an average RMSE of 12.6368, a MAE of 8.1779, and coefficient of determination value of 0.8722.

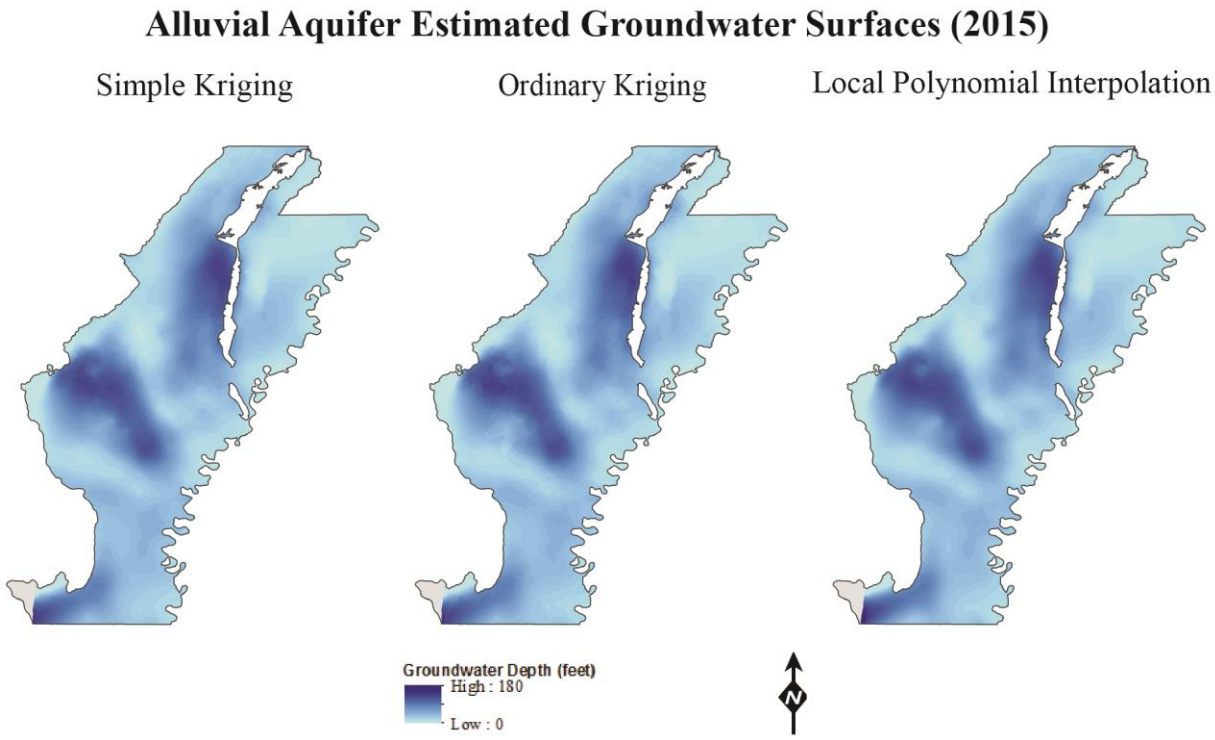

Figure 19. This figure displays the estimated groundwater surfaces generated from simple kriging, ordinary kriging, and local polynomial interpolation methods in 2015

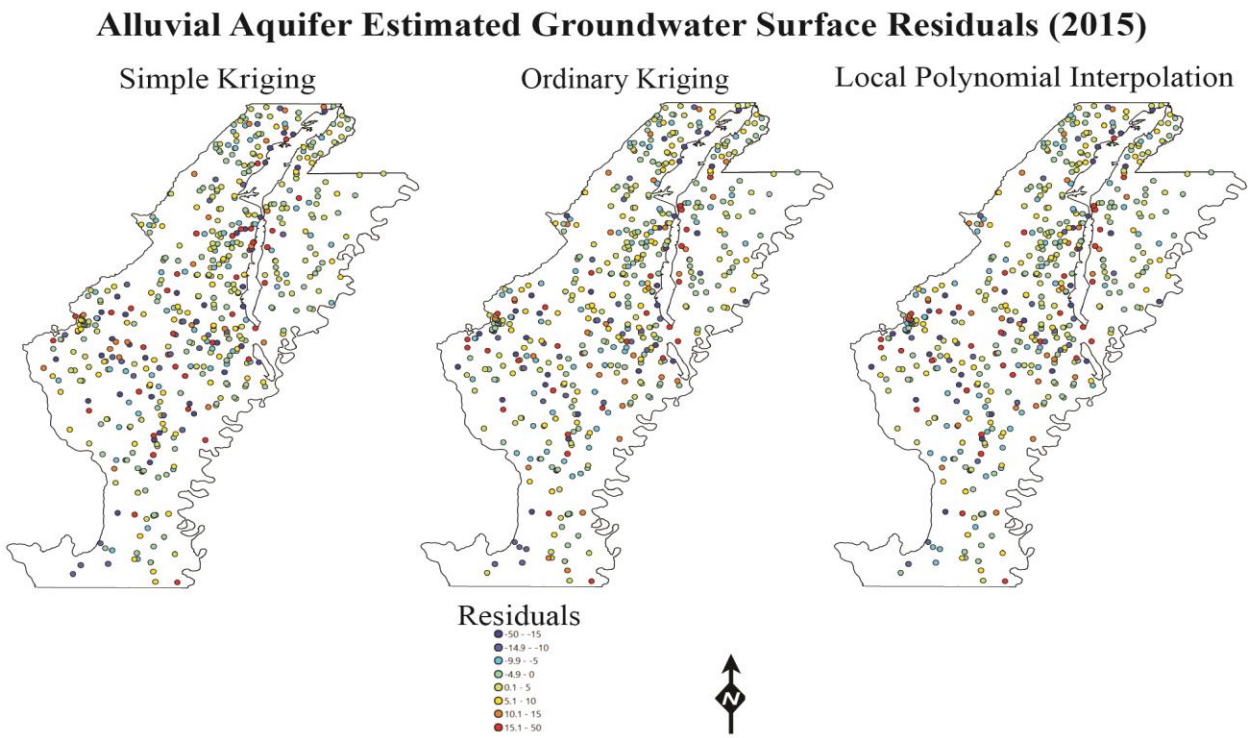

Figure 20. This figure displays the residuals spatially yielded by simple kriging, ordinary kriging, and local polynomial interpolation methods in 2015

Table 21. 2015 Leave-out One Cross Validation

2015 Leave-out One Cross Validation			
Spatial Interpolation Model	RMSE	MAE	R^2
Ordinary Kriging	12.189	7.9512	0.8806
Universal Kriging	13.767	9.047	0.8477
Empirical Bayesian Kriging	12.3048	8.0067	0.8782
Simple Kriging	12.1559	7.8235	0.8812
IDW	12.7973	7.9462	0.8681
Tension Spline	12.9461	8.0754	0.8662
Regularized Spline	13.222	8.3663	0.8608
Local Polynomial Interpolation	12.293	7.9894	0.8784
Global Polynomial Interpolation	23.5869	14.7855	0.5991
Diffusion Interpolation with Barriers	13.6257	8.9896	0.8523
Kernel Interpolation with Barriers	12.1771	8.094	0.8824
Multiquadric Spline	12.6111	7.7713	0.8719
Inverse Multiquadric Spline	13.2089	8.3559	0.8613
Thin Plate Spline	13.0472	8.119	0.8649

Table 22. 2015 k-Fold Cross Validation

2015 k-Fold Cross Validation			
Spatial Interpolation Model	RMSE	MAE	R^2
Ordinary Kriging	12.8306	8.2542	0.8692
Universal Kriging	14.5064	9.5255	0.8334
Empirical Bayesian Kriging	13.1879	8.2724	0.8620
Simple Kriging	12.8408	8.1646	0.8690
IDW	13.5710	8.3687	0.8535
Tension Spline	13.8500	8.5495	0.8494
Regularized Spline	14.1467	8.7830	0.8436
Local Polynomial Interpolation	12.9806	8.3664	0.8660
Global Polynomial Interpolation	21.9578	14.2423	0.6356
Nearest Neighbor	13.2216	N/A	0.8612
IDW with Barriers	14.0266	8.3843	0.8443
Spline with Barriers	13.6648	8.3290	0.8543
Diffusion Interpolation with Barriers	13.9416	9.1828	0.8470
Kernel Interpolation with Barriers	12.7310	8.3946	0.8733
Multiquadric Spline	13.3338	8.2544	0.8586
Inverse Multiquadric Spline	14.1921	8.8104	0.8429
Thin Plate Spline	14.0678	8.6837	0.8543

4.5.1. 2015 CROWLEY'S RIDGE BUFFER

For the Crowley's Ridge Scenario, spline with barriers interpolation method produced the estimated surface with the highest statistical accuracy in 2015. The k-Fold prediction errors yielded were a RMSE of 10.396 and MAE of 7.108, while generating an average coefficient of determination value of 0.923. IDW with barriers produced the surface with the second highest statistical accuracy, yielding a k-Fold RMSE of 10.562, a MAE of 6.854, and coefficient of determination value of 0.919. The kernel interpolation with barriers method produced the surface with the third highest statistical accuracy, yielding a k-Fold cross validation RMSE of 10.418, a MAE of 6.79, and coefficient of determination value of 0.922.

Table 23. 2015 Leave-out One Cross Validation Crowley's Ridge

2015 Leave-out One Cross Validation			
Spatial Interpolation Model	RMSE	MAE	R^2
Ordinary Kriging	11.9782	8.1275	0.8957
Universal Kriging	13.6157	9.1656	0.8653
Empirical Bayesian Kriging	11.4116	7.5823	0.9053
Simple Kriging	11.8928	7.9348	0.8972
IDW	11.1929	7.4895	0.9092
Tension Spline	11.4257	7.4712	0.9055
Regularized Spline	11.6464	7.6411	0.9019
Local Polynomial Interpolation	11.7642	7.8781	0.8994
Global Polynomial Interpolation	16.7274	12.3407	0.7967
Diffusion Interpolation with Barriers	10.9352	7.3607	0.9138
Kernel Interpolation with Barriers	10.2759	6.7277	0.9235
Multiquadric Spline	11.5466	7.4257	0.9031
Inverse Multiquadric Spline	11.6007	7.6261	0.9028
Thin Plate Spline	11.4431	7.5207	0.9053

Table 24. 2015 k-Fold Cross Validation Crowley's Ridge

2015 k-Fold Cross Validation			
Spatial Interpolation Model	RMSE	MAE	R^2
Ordinary Kriging	11.9496	8.3646	0.8973
Universal Kriging	13.6841	9.3744	0.8661
Empirical Bayesian Kriging	11.6234	7.8142	0.9033
Simple Kriging	11.9036	7.9914	0.8981
IDW	11.2690	7.6673	0.9094
Tension Spline	11.3898	7.7523	0.9065
Regularized Spline	11.6558	7.9577	0.9023
Local Polynomial Interpolation	12.0081	8.0877	0.8967
Global Polynomial Interpolation	16.6080	12.1848	0.8021
Nearest Neighbor	11.7574	7.9614	0.9011
IDW with Barriers	10.5616	6.8542	0.9199
Spline with Barriers	10.3959	7.1078	0.9230
Diffusion Interpolation with Barriers	10.9134	7.4368	0.9159
Kernel Interpolation with Barriers	9.9582	6.7957	0.9296
Multiquadric Spline	11.5381	7.7506	0.9046
Inverse Multiquadric Spline	11.6321	7.9469	0.9027
Thin Plate Spline	11.4377	7.7844	0.9230

4.6. FURTHER ANALYSIS

The estimated mean groundwater level in twenty-five out of twenty-nine counties yield declines from 1995 to 2015. In addition, Cleveland, Cross, Poinsett, St. Francis, Desha, Greene, Prairie, Craighead counties all experienced estimated mean groundwater level declines in excess of 8.4 feet. A Pearson's correlation test was conducted on the county estimated mean groundwater level change occurring from 1995 to 2015 and the mean groundwater usage rate 1995 to 2010. The correlation test generated a p-value of 0.0354, which leads to the rejection of the null hypothesis that the two variables are uncorrelated.

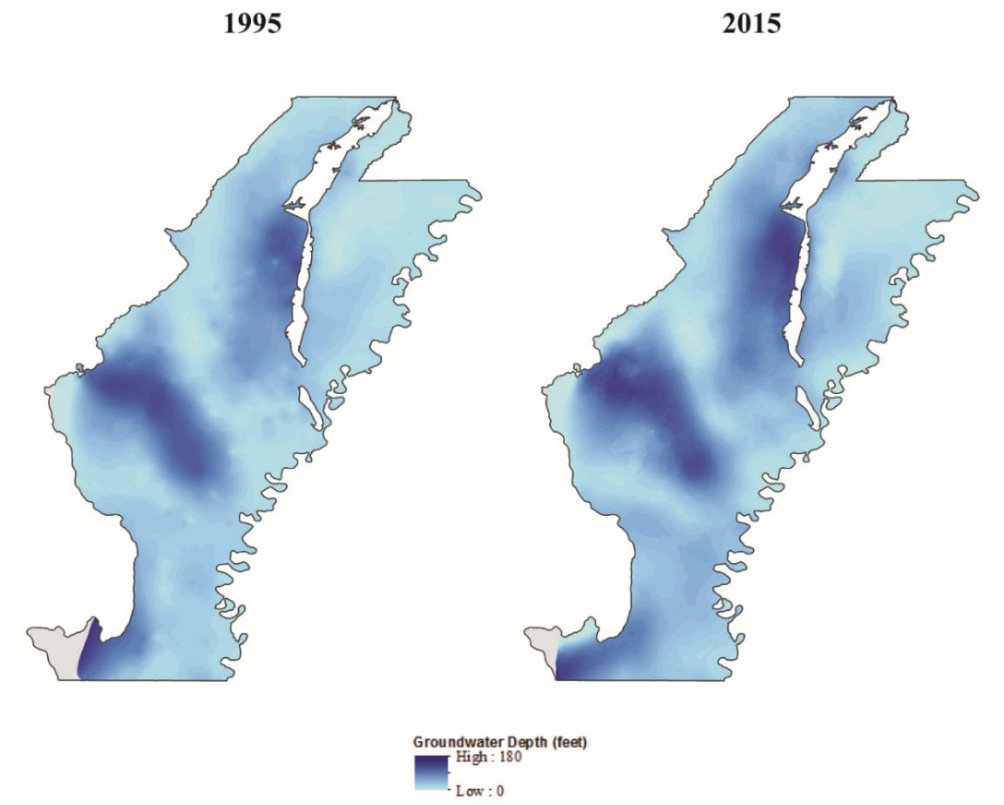

Figure 21. This figure displays 1995 and 2015 estimated groundwater surfaces generated from ordinary kriging. The 2015 surface demonstrates a significant increase in groundwater depth.

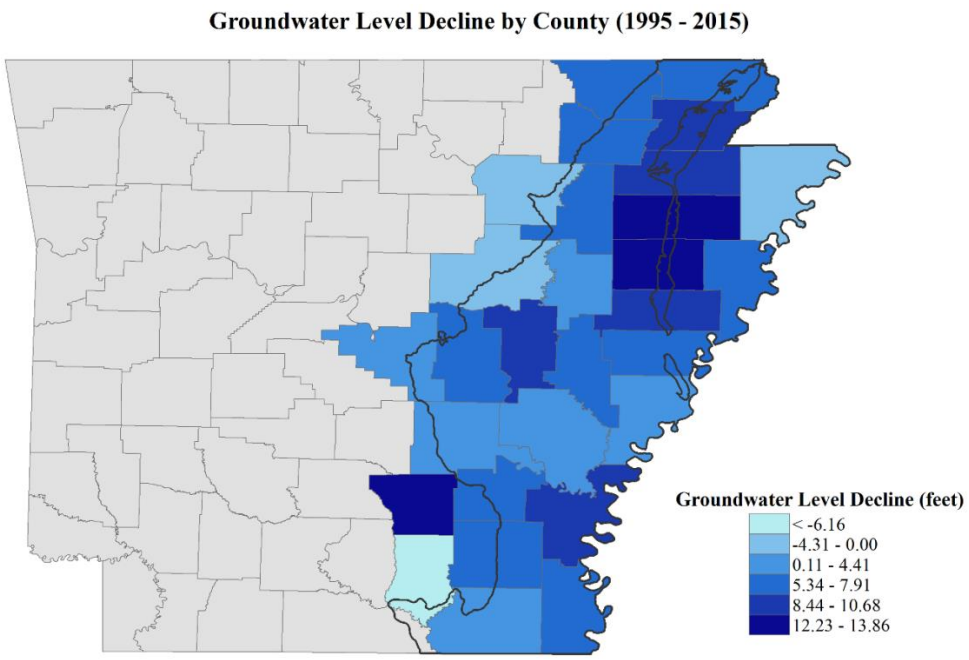

Figure 22. This figure shows the estimated mean groundwater level changes occurring from 1995 to 2015

5. Discussion and Conclusion

5.1. Summary of Research Questions

The primary research question of this study was to determine which spatial interpolation method serves as the optimal method for modeling groundwater levels in the Mississippi River Valley Alluvial Aquifer. Based upon the results of two types of cross-validation for five separate years, ordinary kriging is the most appropriate interpolation method for generating groundwater level estimations for this particular study area. Simple kriging and empirical Bayesian kriging also provide suitable methods for producing groundwater level estimations for the Mississippi River Valley Alluvial Aquifer.

Ordinary kriging produced estimated surfaces with the highest statistical accuracy throughout the study. The average prediction errors yielded were a RMSE of 10.518 and MAE of 7.042, while generating an average coefficient of determination value of 0.89. Within the Crowley's Ridge study area, ordinary kriging produced the surfaces with an average RMSE of 9.156, a MAE of 6.87, and coefficient of determination value of 0.905.

Simple kriging produced estimated surfaces with the second highest statistical accuracy throughout the study. The average prediction errors yielded were a RMSE of 10.689 and MAE of 7.129, while generating an average coefficient of determination value of 0.886. Within the Crowley's Ridge study area, simple kriging produced the surfaces with an average RMSE of 10.077, a MAE of 6.888, and coefficient of determination value of 0.902. The RMSE value yielded by simple kriging within the Crowley's ridge study area was significantly higher than the RMSE value yielded by ordinary kriging.

Empirical Bayesian kriging produced estimated surfaces with the third highest statistical accuracy throughout the study. The average prediction errors yielded were a RMSE of 10.556

and MAE of 6.931, while generating an average coefficient of determination value of 0.889. Within the Crowley's Ridge study area, empirical Bayesian kriging produced the surfaces with an average RMSE of 9.705, a MAE of 6.399, and coefficient of determination value of 0.908. These results demonstrated a significant amount of more accuracy within the Crowley's Ridge study area than both ordinary and simple kriging.

However, spline with barriers was the interpolation method that produced the highest accuracy within the Crowley's Ridge study area. The average prediction errors yielded were a RMSE of 8.776 and MAE of 5.849, while generating an average coefficient of determination value of 0.926. Throughout the complete study area the average prediction errors yielded by spline with barriers were a RMSE of 10.987 and MAE of 6.947, while generating an average coefficient of determination value of 0.882. These prediction errors are comparable to those yielded by empirical Bayesian kriging.

Additionally, the number of trials is a critical factor in determining the significance of the differences in RMSE values. If there had only been one trial, the differences in RMSE values would have been insignificant. However, the difference was indeed significant as the RMSE values were averaged over five separate years. Overall, there are a total of four to five interpolation methods which performed successfully in a consistent manner, hence it is appropriate to consider them suitable. Contrastingly, there were three to four interpolation methods that consistently performed poorly.

An intriguing trend in this study's results was a general trend towards lower statistical accuracy in the interpolation surfaces as the years went and I believe this is a direct result of increased variation in groundwater depth measurements. As a result, determining which interpolation method is the most appropriate going forward is essential. In addition, IDW and

Natural Neighbor, the methods employed by the Arkansas Geological Survey and the Arkansas Natural Resource Commission did not factor in the factor into the most accurate methods and actually were some of the interpolation methods yielding some of the lowest statistical accuracy in this case study.

The second research question was have the fluctuations in the alluvial aquifer's groundwater levels exhibited a noticeable general trend of decline in recent history? A general trend of groundwater depletion is confirmed by twenty-five out of twenty-nine counties yielding declines in their estimated mean groundwater level from 1995 to 2015 and eight counties experiencing mean groundwater level declines in excess of 8.4 feet. The third research question for this study was does the majority of the study area's counties exhibit a significantly similar interaction between groundwater level changes and the varying rates of groundwater withdrawals associated with particular counties? This notion was confirmed by a Pearson's correlation test generating a p-value of 0.0354 leading to the rejection of the null hypothesis that the two variables are uncorrelated.

5.2. Limitations and Areas for Future Study

The primary limitation of this case study was the general lack of groundwater measurements in neighboring states in close proximity to the Arkansas border. Mississippi provided significant amounts groundwater measurements from 1995 to 2010; however, in 2015 the spatial coverage of groundwater measurements in Mississippi fell below ten measurements. The remaining neighboring states produced unsatisfactory amounts of groundwater measurements throughout the case study.

A future area of study would be to generate a predictive model to groundwater levels in the study area. This model could potentially take numerous variables that affect groundwater

levels into consideration. Examples of the potential variables include, confining unit thickness, aquifer thickness, proximity to major rivers, precipitation averages, soil properties, elevation, groundwater flow patterns, trends in groundwater levels and water usage.

Another, potential area of future study would be the creation of a tool that would employ the same notions utilized in this respective case study that would automate a large portion of the work involved. This tool could prove to be very useful in groundwater monitoring in the near future. Based up on the current availability of groundwater depth measurements, I believe that this tool could potentially create a new groundwater level surface every six months for monitoring purposes.

REFERENCES

Bailey, T. C., & Gatrell, A. C. (1995). *Interactive Spatial Data Analysis*. Longman Scientific & Technical.

Bohling, G. (2005). *Kriging*. Retrieved from http://people.ku.edu/~gbohling

Burrough, P. A., & McDonnell, R. A. (1998). *Principles of Geographical Information Systems* (2nd ed.). Oxford University Press.

Charoenpong, S., Suwanprasit, C., & Thongchumnum, P. (2012). Impacts of Interpolation Techniques on Groundwater Potential Modeling Using GIS in Phuket Province, Thailand. *ANdaman Environment and Natural Disaster Research Center*.

Chenoweth, M. E. (2009). A Numerical Study of Generalized Multiquadric Radial Basis Function Interpolation. *Marshall University*. Retrieved from https://www.siam.org/students/siuro/vol2issue2/S01040.pdf

Childs, C. (2004). Interpolating Surfaces in ArcGIS Spatial Analyst. *ESRI Education Services*. Retrieved from https://www.esri.com/news/arcuser/0704/files/interpolating.pdf

Clark, B., Westerman, D., & Fugitt, T. (2013). *Enhancements to the Mississippi Embayment Regional Aquifer Study (MERAS) Groundwater-Flow Model and Simulations of Sustainable Water-Level Scenarios* (No. 5161). United States Geological Survey. Retrieved from http://pubs.usgs.gov/sir/2013/5161/pdf/sir2013-5161.pdf

Czarnecki, J., Hays, P., & Paul, M. (2002). *The Mississippi River Valley Alluvial Aquifer in Arkansas:A Sustainable Water Resource?* United States Geological Survey. Retrieved from http://ar.water.usgs.gov/LOCAL_REPORTS/FS-041-02.pdf

Czarnecki, J., Clark, B., & Stanton, G. (2003). *Conjunctive Use Optimization Model of the Mississippi River Valley Alluvial Aquifer of Southeastern Arkansas* (Water-Resources Investigations Report No. 4233). United States Geological Survey. Retrieved from http://pubs.usgs.gov/wri/wri034233/WRIR03-4233.pdf

Engler, K., & Bayley, F. H. (1963). *Artificial Recharge of Ground Water Grand Prairie Region, Arkansas*. United States Department of the Interior. Retrieved from http://pubs.usgs.gov/wsp/1615a/report.pdf

Engler, K., Thompson, D. G., & Kazmann, R. G. (1945). Ground-water supplies for rice irrigation in the Grand Prairie region, Arkansas. *University of Arkansas Agricultural Experiment Station, 457*.

Flanders, A. (2014). Input Costs Trends for Arkansas Field Crops, 2008-2014. *Department of Agricultural Economics and Agribusiness University of Arkansas*. Retrieved from http://www.uaex.edu/farm-ranch/economics-marketing/farm-planning/FlandersInputCosts_Augt2014.pdf

Gates, J. (2005). Groundwater Irrigation in the Development of the Grand Prairie Rice Industry, 1896-1950. *University of Nebraska*. Retrieved from http://digitalcommons.unl.edu/cgi/viewcontent.cgi?article=1173&context=geosciencefacpub

Ground Water Atlas of the United States. (n.d.). Retrieved from http://pubs.usgs.gov/ha/ha730/ch_f/F-surficial.html

Halberg, H. N. (1972). *Use of Water in Arkansas, 1970*. United States Geological Survey. Retrieved from http://www.geology.ar.gov/pdf/Water%20Resources%20Summary%207_v.pdf

How Diffusion Interpolation with Barriers works. (n.d.). Retrieved from http://pro.arcgis.com/en/pro-app/help/analysis/geostatistical-analyst/how-diffusion-interpolation-with-barriers-works.htm

How Radial Basis Functions (RBF) work. (2007). Retrieved from http://webhelp.esri.com/arcgisdesktop/9.2/index.cfm?TopicName=How_Radial_Basis_Functions_(RBF)_work

How Spline with Barriers works. (n.d.). Retrieved from http://desktop.arcgis.com/en/arcmap/10.3/tools/spatial-analyst-toolbox/how-spline-with-barriers-works.htm

Jamil, R. M., Said, M. N., & Reba, M. N. (2011). Geostatistics approach with indicator kriging for assessing groundwater vulnerability to Nitrate contamination. *7th Esri Asia Pacific User Conference*. Retrieved from http://umkeprints.umk.edu.my/1008/1/Geostatistics%20Approach.pdf

Javaran, H., & Khaji, N. (2012). Inverse Multiquadric (IMQ) function as radial basis function for plane dynamic analysis using dual reciprocity boundary element method. *Tarbiat Modares University*.

Kernel Interpolation With Barriers. (n.d.). Retrieved from http://pro.arcgis.com/en/pro-app/tool-reference/geostatistical-analyst/Kernel-interpolation-with-barriers.htm

Kettle, N., Harrington, L., & Harrington, J. (n.d.). Groundwater Depletion and Agricultural Land Use Change in Wichita County, Kansas. *The Professional Geographer*, *59*(2). Retrieved from https://krex.k-state.edu/dspace/bitstream/handle/2097/4947/KettlePG2007.pdf?sequence=1

Khazaz, L., Oulidi, H. J., Moutaki, S. E., & Ghafiri, A. (2015). Comparing and Evaluating Probabilistic and Deterministic Spatial Interpolation Methods for Groundwater Level of Haouz in Morocco. *Journal of Geographic Information Syste*, *7*, 631–64.

Konikow, L. F. (2013). *Groundwater Depletion in the United States (1900−2008)* (Scientific Investigations Report No. 5079). United States Geological Survey. Retrieved from http://pubs.usgs.gov/sir/2013/5079/SIR2013-5079.pdf

Krivoruchko, K. (2012). Empirical Bayesian Kriging Implemented in ArcGIS Geostatistical Analyst. *Esri*. Retrieved from http://www.esri.com/news/arcuser/1012/files/ebk.pdf

Kumar, V., & Remadavi. (2006). Kriging of Groundwater Levels – A Case Study. *Journal of Spatial Hydrology*, *6*(1).

Mahon, G., & Ludwig, A. H. (1990). *Simulation of Ground-Water Flow in the Mississippi River Valley Alluvial Aquifer in Eastern Arkansas* (Water-Resources Investigations Report No. 4145). Retrieved from http://pubs.usgs.gov/wri/1989/4145/report.pdf

Mahon, G. L., & Poynter, D. T. (1993). *Development, Calibration, and Testing of Ground-Water Flow Models for the Mississippi River Valley Alluvial Aquifer in Eastern Arkansas Using One-Square-Mile Cells* (Water-Resources Investigations Report No. 4106). United States Geological Survey. Retrieved from http://pubs.usgs.gov/wri/1992/4106/report.pdf

Maupin, M. A., Kenny, J. F., & Hutson, S. S. (2014). *Estimated Use of Water in the United States in 2010*. United States Geological Survey. Retrieved from http://pubs.usgs.gov/circ/1405/pdf/circ1405.pdf

National Agriculture Statistics Service. CropScape and Cropland Data Layer. (n.d.). Retrieved from https://www.nass.usda.gov/Research_and_Science/Cropland/SARS1a.php

National Agriculture Statistics Service. Data and Statistics. (n.d.). Retrieved from https://www.nass.usda.gov/Statistics_by_State/Arkansas/index.php

Olea, R. (2009). *A Practical Primer on Geostatistics* (Open-File Report No. 1103). United States Geological Survey. Retrieved from https://pubs.usgs.gov/of/2009/1103/ofr2009-1103-rev-jan2010.pdf

Pugh, A. L., & Holland, T. W. (2015). *Estimated Water Use in Arkansas, 2010* (Scientific Investigations Report No. 5062). United States Geological Survey. Retrieved from http://pubs.usgs.gov/sir/2015/5062/pdf/sir2015-5062.pdf

Rabah, F., Ghabayen, S., & Salha, A. (2011). Effect of GIS Interpolation Techniques on the Accuracy of the Spatial Representation of Groundwater Monitoring Data in Gaza Strip. *Journal of Environmental Science and Technology*, *4*(6), 579–589. Retrieved from http://www.scialert.net/abstract/?doi=jest.2011.579.589

Rice Production in Arkansas. (n.d.). Retrieved from http://www.uaex.edu/farm-ranch/crops-commercial-horticulture/rice/

RMS Error. (n.d.). Retrieved from http://support.esri.com/other-resources/gis-dictionary/term/RMS%20error

Rogerson, P. A. (2015). *Statistical Methods for Geography: A Student's Guide* (4th ed.). SAGE Publications Ltd.

R-squared. (n.d.). Retrieved from http://support.esri.com/sitecore/content/support/Home/other-resources/gis-dictionary/term/r-squared

Salah, H. (2009). Geostatistical analysis of groundwater levels in the south Al Jabal Al Akhdar area using GIS. *GIS Ostrava*, *25*. Retrieved from http://gis.vsb.cz/GIS_Ostrava/GIS_Ova_2009/sbornik/Lists/Papers/005.pdf

Schrader, T. P. (2001). *Status of Water Levels and Selected Water-Quality Conditions in the Mississippi River Valley Alluvial Aquifer in Eastern Arkansas, 2000* (Water-Resources Investigations Report No. 4124). United States Geological Survey. Retrieved from http://pubs.usgs.gov/wri/2001/4124/report.pdf

Schrader, T. P. (2008). *Water Levels and Selected Water-Quality Conditions in the Mississippi River Valley Alluvial Aquifer in Eastern Arkansas, 2006* (Scientific Investigations Report No. 5092). United States Geological Survey. Retrieved from http://pubs.usgs.gov/sir/2008/5092/pdf/SIR2008-5092.pdf

Sun, Y., Kang, S., Li, F., & Zhang, L. (2009). Comparison of interpolation methods for depth to groundwater and its temporal and spatial variations in the Minqin oasis of northwest China. *Environmental Modelling & Software*, *24*(10).

Swaim, E. (2014). *The Arkansas Groundwater Protection and Management Report 2013*. Arkansas Natural Resources Commission. Retrieved from https://static.ark.org/eeuploads/anrc/2013-2014AnnualReport.pdf

Tamayo, S. (2012). On the Use of Weighted Mean Absolute Error in Recommender Systems. *RECSYS*. Retrieved from https://www.semanticscholar.org/paper/On-the-Use-of-Weighted-Mean-Absolute-Error-in-Cleger-Tamayo-Fern%C3%A1ndez-Luna/2ce9be7c7698607808fe54f90eae9cfce89da29c/pdf

The 50th Anniversary of GIS. (2012). Retrieved from http://www.esri.com/news/arcnews/fall12articles/the-fiftieth-anniversary-of-gis.html

Tullis, J.A., Cothren, J.D., Lanter D.P., Shi, X., Limp, W.F., Linck, R.F., ….Alsumaiti, T.S. (2016). *In Remotely Sensed Data Characterization, Classification, and Accuracies.* Taylor & Francis Group, LLC.

United States Geological Survey. Current Water Data for Arkansas. (n.d.). Retrieved from http://waterdata.usgs.gov/ar/nwis/rt

Yamamoto, J. K. (2005). Correcting the Smoothing Effect of Ordinary Kriging Estimates. *Mathematical Geology*, *37*(1), 69–94.

Yao, L., Huo, Z., Feng, S., Mao, X., Kang, S., Chen, J., … Steenhius, T. (2013). Evaluation of spatial interpolation methods for groundwater level in an arid inland oasis, northwest China. *Environ Earth Sci*, *71*, 1911–1924.

APPENDIX A – MODELBUILDER MODELS

As described in section 3.3.1, the majority of the data preprocessing accomplished via ModelBuilder Models. These particular models are utilized to employ 10 fold cross validation.

A.1. MODEL 1, PART 1

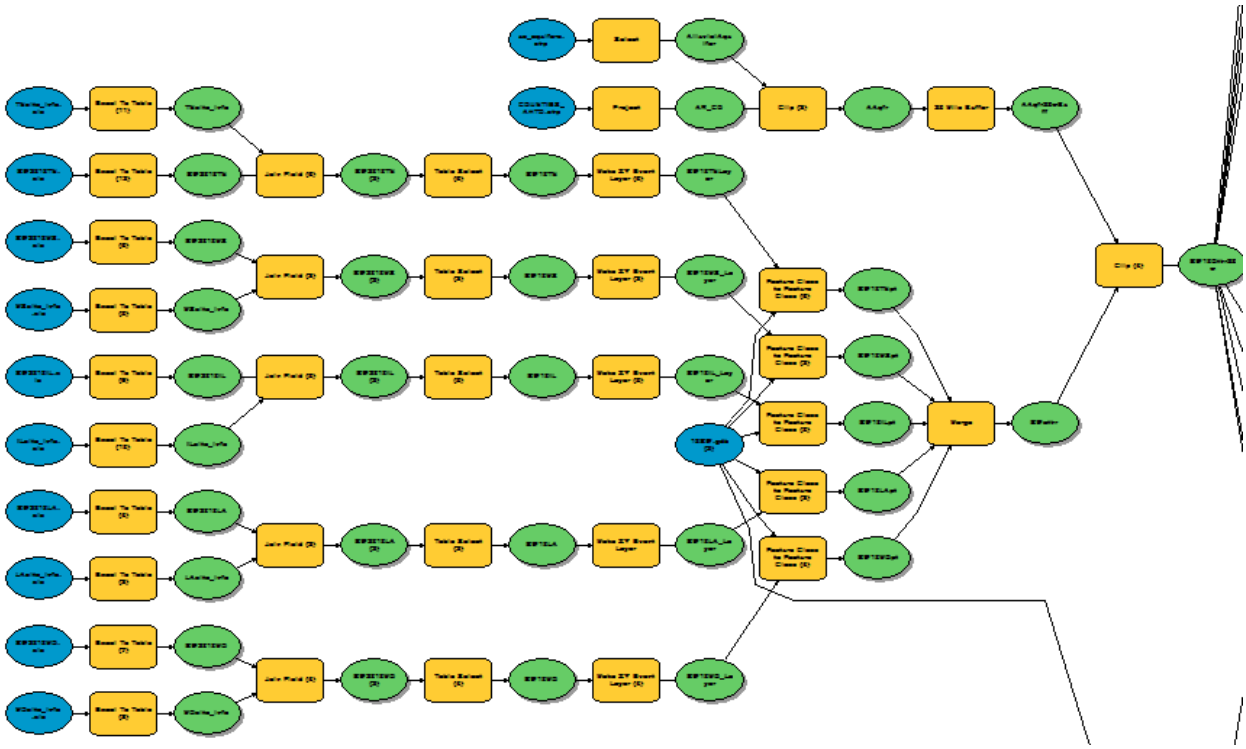

This portion of the model consists of merging and joining several excel files, which are later projected relative to their latitude and longitude values. These files represent groundwater values in neighboring states. Utilizing the clipping tool values that fall outside of 25 mile buffer of Arkansas are removed.

A.2. MODEL 1, PART 2

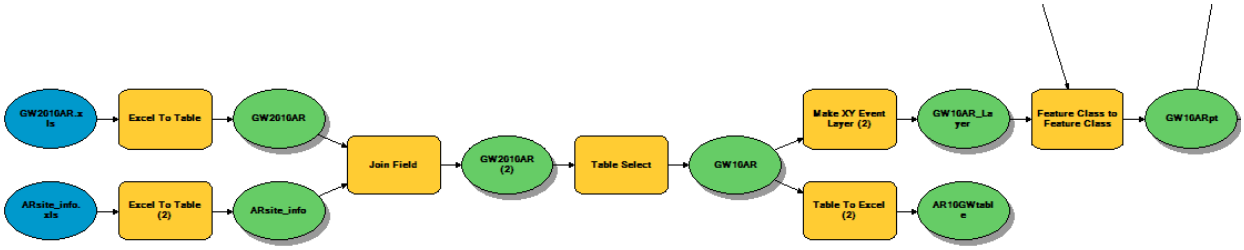

Similar to part one, this portion of the model consists of merging and joining two excel files, which are then projected relative to their latitude and longitude values. These excel spreadsheets contain groundwater depth values, all of which are utilized in this study.

A.3. MODEL 1, PART 3

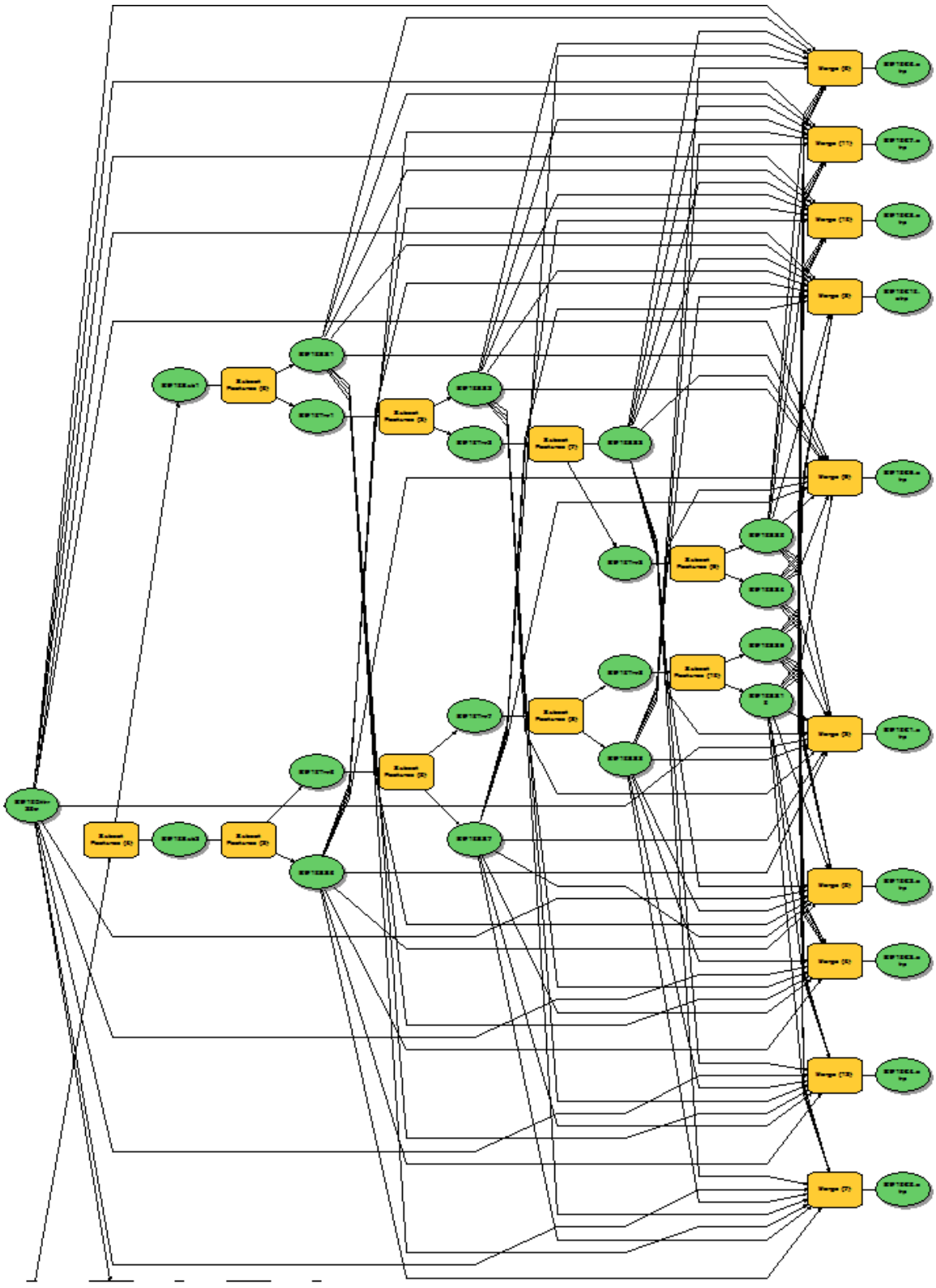

The third portion of the first model demonstrates the partitioning of the groundwater depth values into ten different subsets to later be utilized in k-fold cross-validation.

A.4. MODEL 2

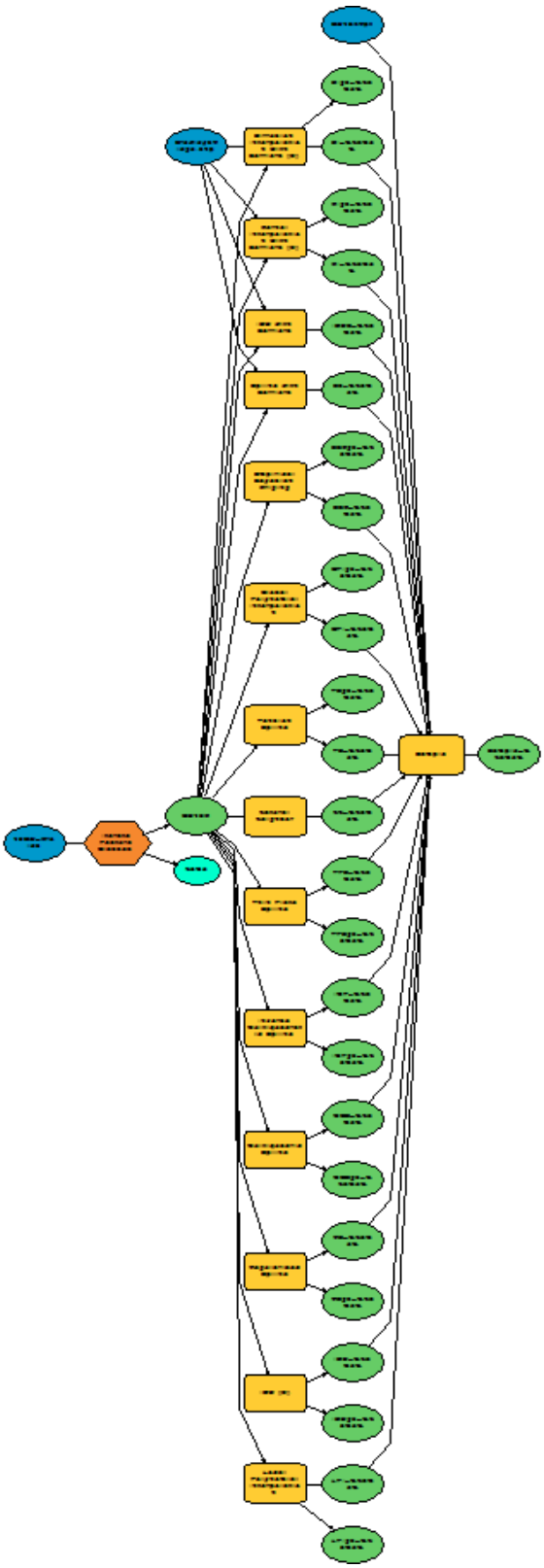

The second model is the process of iterating and generating interpolated surfaces utilizing the ten previously established subsets.

A.5. MODEL 3, PART 1

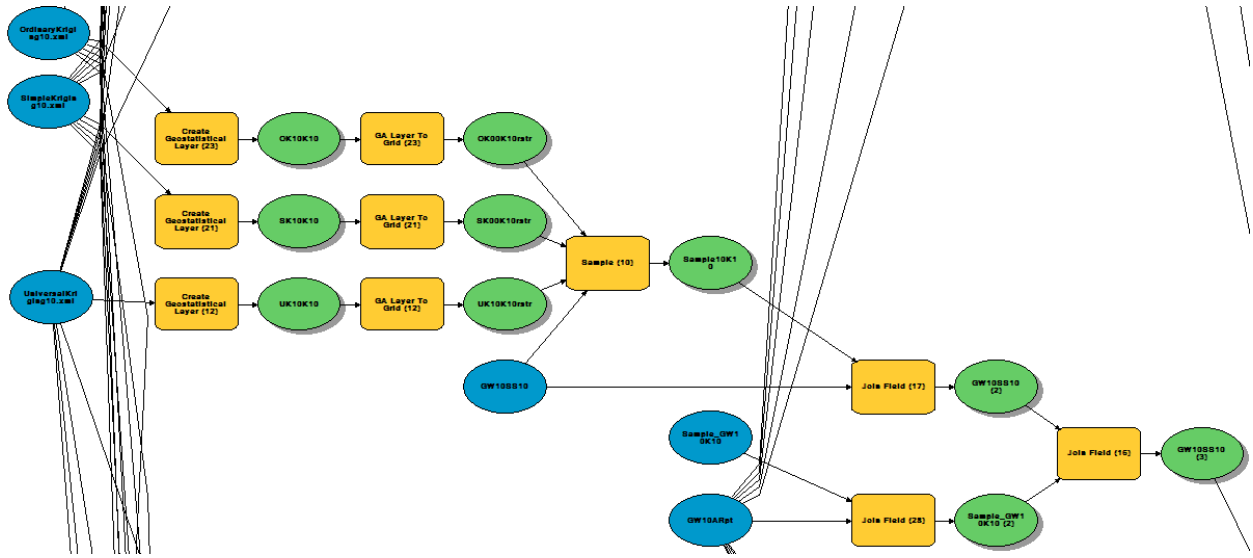

This portion of the third model shows the sampling of estimated values relative to the subset withheld during estimation.

A.6. MODEL 3, PART 2

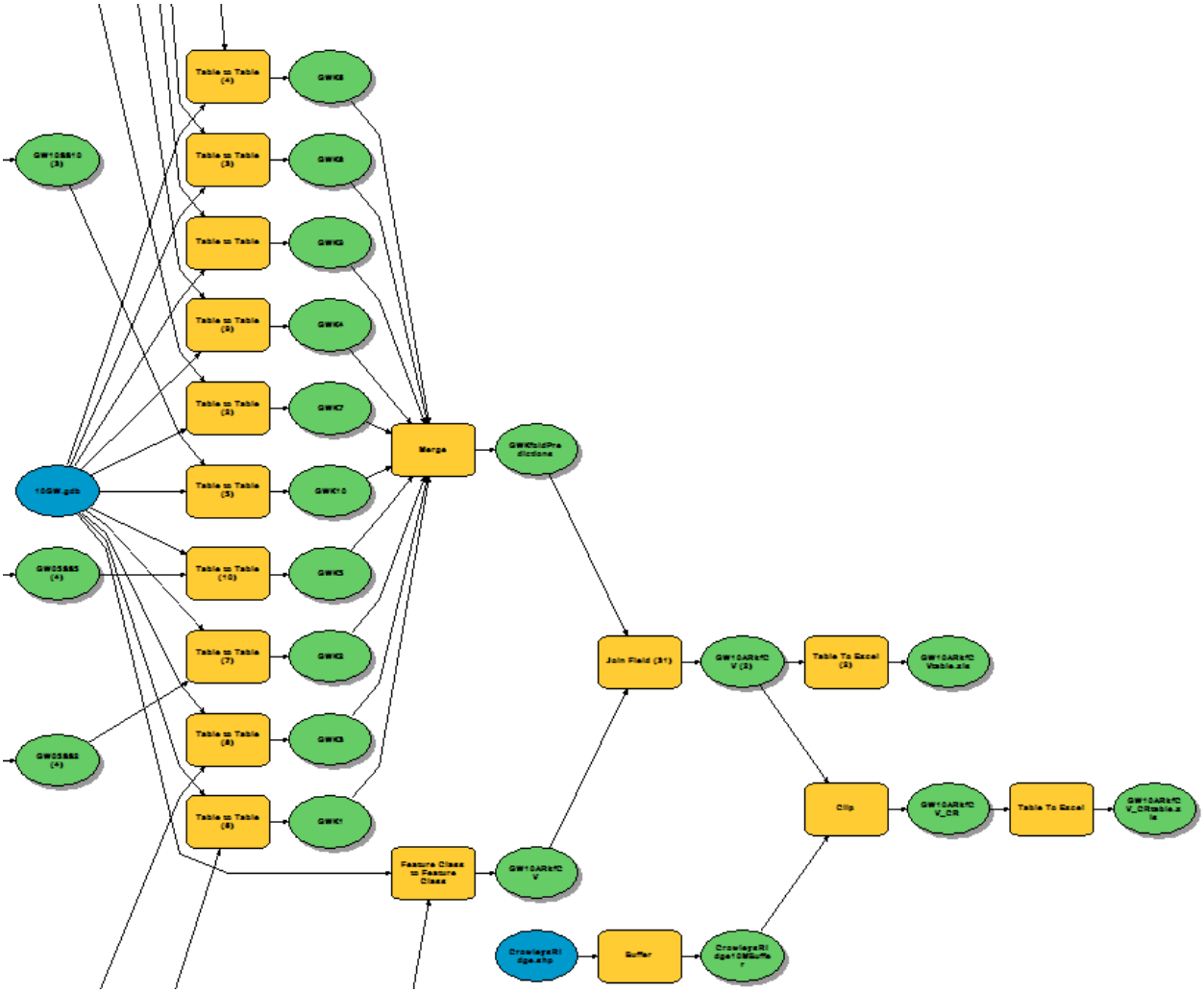

The second portion of the third model demonstrates the ten withheld subset samples being merged and joined together. These tables are then exported into an excel spreadsheet format.

APPENDIX B – RSTUDIO CROSS-VALIDATION SCRIPT

As stated in section 3.3.2., RStudio was employed repeatedly for various purposes related to statistical computation. The following script was employed for conduction cross-validation statistics, which were utilized for to conduct a comparative analysis of the accuracy of surface estimations.

B.1. CROSS-VALIDATION R SCRIPT

```
GW10ARkfCVtable <- read.csv("W:/jolilly/aqufr/10GWtables/GW10ARkfCVtable.csv")
attach(GW10ARkfCVtable)


#test dataset
obs <- lev_va #Observed Values


#Interpolated Values
RS <- RS
LPI <- LPI
IDW <- IDW
IDWB <- IDWB
TS <- TS
OK <- OK
NN <- NN
UV <- UK
EK <- EBK
SK <- SK
SB <- SB
DI <- DI
KI <- KI
MQS <- MQS
GPI <- GPI
IMF <- IMF
MQS <- MQS
TPS <- TPS



# Function that returns Root Mean Squared Error
rmse <- function(error)
{
  sqrt(mean((error)^2, na.rm =TRUE))
```

```
}


# Function that returns Mean Absolute Error
mae <- function(error)
{
  mean(abs(error))
}



#Caculate Error
#error <- Simulated - Observed
RS.er <- RS - obs
LPI.er <-  LPI - obs
IDW.er <- IDW - obs
TS.er <- TS - obs
GPI.er <-  GPI - obs
OK.er <-  OK - obs
NN.er <-  NN - obs
UV.er <-  UV - obs
EK.er <-  EK - obs
SK.er <- SK - obs
IDWB.er <- IDWB - obs
SB.er <- SB - obs
DI.er <- DI - obs
KI.er <- KI - obs
IMF.er <- IMF - obs
MQS.er <- MQS - obs
TPS.er <- TPS - obs

#RMSE Calculations
OK.rmse <- rmse(OK.er)
UV.rmse <- rmse(UV.er)
EK.rmse <- rmse(EK.er)
IDW.rmse <- rmse(IDW.er)
RS.rmse <- rmse(RS.er)
TS.rmse <- rmse(TS.er)
LPI.rmse <- rmse(LPI.er)
GPI.rmse <- rmse(GPI.er)
NN.rmse <- rmse(NN.er)
SK.rmse <- rmse(SK.er)
IDWB.rmse <- rmse(IDWB.er)
SB.rmse <- rmse(SB.er)
DI.rmse <- rmse(DI.er)
KI.rmse <- rmse(KI.er)
```

```
IMF.rmse <- rmse(IMF.er)
MQS.rmse <- rmse(MQS.er)
TPS.rmse <- rmse(TPS.er)


#MAE Calculations
OK.mae <- mae(OK.er)
UV.mae <- mae(UV.er)
EK.mae <- mae(EK.er)
IDW.mae <- mae(IDW.er)
RS.mae <- mae(RS.er)
TS.mae <- mae(TS.er)
LPI.mae <- mae(LPI.er)
GPI.mae <- mae(GPI.er)
NN.mae <- mae(NN.er)
SK.mae <- mae(SK.er)
MQS.mae <- mae(MQS.er)
SB.mae <- mae(SB.er)
DI.mae <- mae(DI.er)
KI.mae <- mae(KI.er)
IMF.mae <- mae(IMF.er)
MQS.mae <- mae(MQS.er)
TPS.mae <- mae(TPS.er)
IDWB.mae <- mae(IDWB.er)

#Coefficient of Determination r^2
OK.lm <- lm(obs ~ OK)
UV.lm <- lm(obs ~ UV)
EK.lm <- lm(obs ~ EK)
IDW.lm <- lm(obs ~ IDW)
TS.lm <- lm(obs ~ TS)
RS.lm <- lm(obs ~ RS)
LPI.lm <- lm(obs ~ LPI)
GPI.lm <- lm(obs ~ GPI)
NN.lm <- lm(obs ~ NN)
SK.lm <- lm(obs ~ SK)
IDWB.lm <- lm(obs ~ IDWB)
SB.lm <- lm(obs ~ SB)
DI.lm <- lm(obs ~ DI)
KI.lm <- lm(obs ~ KI)
IMF.lm <- lm(obs ~ IMF)
MQS.lm <- lm(obs ~ MQS)
TPS.lm <- lm(obs ~ SB)

OK.r2 <- summary(OK.lm)$r.squared
UV.r2 <- summary(UV.lm)$r.squared
```

```
EK.r2 <- summary(EK.lm)$r.squared
IDW.r2 <- summary(IDW.lm)$r.squared
TS.r2 <- summary(TS.lm)$r.squared
RS.r2 <- summary(RS.lm)$r.squared
LPI.r2 <- summary(LPI.lm)$r.squared
GPI.r2 <- summary(GPI.lm)$r.squared
NN.r2 <- summary(NN.lm)$r.squared
SK.r2 <- summary(SK.lm)$r.squared
IDWB.r2 <- summary(IDWB.lm)$r.squared
SB.r2 <- summary(SB.lm)$r.squared
DI.r2 <- summary(DI.lm)$r.squared
KI.r2 <- summary(KI.lm)$r.squared
IMF.r2 <- summary(IMF.lm)$r.squared
MQS.r2 <- summary(MQS.lm)$r.squared
TPS.r2 <- summary(TPS.lm)$r.squared


IntModel <- c("Ordinary Kriging", "Universal Kriging", "Empirical Bayesian Kriging", "Simple
Kriging", "IDW","Tension Spline", "Regularized Spline", "Local Polynomial Interpolation",
"Global Polynomial Interpolation", "Nearest Neighbor", "IDW with Barriers", "Spline with
Barriers", "Diffusion Interpolation with Barriers", "Kernel Interpolation with
Barriers","Multiquadric Spline", "Inverse Multiquadric Spline", "Thin Plate Spline")
Interpolation.RMSE <- c(OK.rmse, UV.rmse, EK.rmse, SK.rmse, IDW.rmse, TS.rmse, RS.rmse,
LPI.rmse, GPI.rmse, NN.rmse, IDWB.rmse, SB.rmse, DI.rmse, KI.rmse, MQS.rmse, IMF.rmse,
TPS.rmse)
Interpolation.mae <- c(OK.mae, UV.mae, EK.mae, SK.mae, IDW.mae,TS.mae, RS.mae,
LPI.mae, GPI.mae, NN.mae, IDWB.mae, SB.mae, DI.mae, KI.mae, MQS.mae, IMF.mae,
TPS.mae)
Interpolation.r2 <- c(OK.r2, UV.r2, EK.r2, SK.r2, IDW.r2, TS.r2, RS.r2, LPI.r2, GPI.r2, NN.r2,
IDWB.r2, SB.r2, DI.r2, KI.r2, MQS.r2, IMF.r2, TPS.r2)

ARGW10_kfoldCV <- data.frame(SpatialInterpolationModel = IntModel, RMSE =
Interpolation.RMSE, MAE =Interpolation.mae, r2= Interpolation.r2)
print(ARGW10_kfoldCV)


write.csv(ARGW10_kfoldCV , file = "W:/jolilly/aqufr/10GWtables/ARGW10_kfoldCV.csv")
```